

SURVEY

Wave Propagation Modeling Techniques in Tunnel Environments: A Survey

MD. ABDUS SAMAD¹, (Member, IEEE), SUNG-WOONG CHOI², (Senior Member, IEEE),
CHUNG-SUP KIM³, AND KWONHUE CHOI¹, (Senior Member, IEEE)

¹Department of Information and Communication Engineering, Yeungnam University, Gyeongsan-si, Gyeongsangbuk-do 38541, South Korea

²Broadcasting & Telecommunication Media Research Laboratory, Electronics and Telecommunications Research Institute, Daejeon 34129, South Korea

³Radio and Satellite Research Division, Radio Resource Research Section, Electronics and Telecommunications Research Institute, Daejeon 34129, South Korea

Corresponding author: Kwonhue Choi (gonew@yu.ac.kr)

This work was supported by the Institute of Information & Communications Technology Planning & Evaluation (IITP) funded by the Korean Government [Ministry of Science and ICT (MSIT)] through the Development of Adaptive Interference Reduction Technology Based on Civil-Military Shared Frequency Environment under Grant 2022-0-00024.

ABSTRACT The prediction of radio signal transmission in tunnels is important for wireless communication link design as it enables the delivery of optimum power to the intended receiver inside the tunnel. Several techniques have been proposed to estimate path loss for wireless communication inside tunnels. The radio coverage range and where base stations need to be installed can be figured out with the help of propagation models. At the time of developing these models, modeling complexity and environmental attributes, such as the tunnel geometry and the electrical and magnetic properties of its walls and interior materials are considered. A limited amount of literature currently overviews how waves transmit through tunnels and how electromagnetic wave transmission has recently changed. This survey, which examines current advancements in the propagation of waves in tunnels, aims to address this gap. In this review, thirty wave propagation models were analyzed and grouped into distinct categories for the first time. The detailed specifications of each model were omitted to make the survey easy to comprehend. This comparative research will help service providers adopt an appropriate propagation model and plan efficient transmitter and receiver placement and link management for a specific tunnel environment.

INDEX TERMS Artificial neural network, radio wave propagation, ray tracing, scaling, tunnel.

I. INTRODUCTION

As societies develop, and the use of tunnels for transportation, mining natural fossils, minerals, or military operations has increased. In addition, we use various telecommunications-based services in our everyday life. Consequently, reliable telecommunication knowledge and radio frequency (RF) propagation prediction inside various types of tunnels are necessary when using tunnels. While commuting through tunnels, commuters desire an uninterrupted telecommunications service. This perspective is critical for mobile-operator services. In addition, a surveillance system connected to the outside through a telecommunications network must be established inside the tunnels for security

The associate editor coordinating the review of this manuscript and approving it for publication was Wei-Wen Hu¹.

purposes. Network infrastructures can also be destroyed, particularly after vehicle accidents and tunnel fires, which force public safety users to interact directly without physical communication. In such instances, it is vital to know the features of the wireless channel at distances beyond the range of the usual tunnel base station. In contrast to wave propagation in an open space, electromagnetic wave propagation in tunnels uses modal decomposition and ray tracing mechanisms as the spaces are closed environments [1].

As an alternative to wireless communication inside tunnels, a leaky feeder technique can be used. Such a type of cable is called leaky because the exterior conductor includes holes or slots that allow radio signals to enter and exit along its length. Consequently, the cable is prone to signal loss. To compensate for the loss of signal, line amplifiers need to be placed at regular intervals, often every 350 to 500 m, to amplify

the signal to an acceptable level. A typical frequency band ranges from 150 MHz to approximately 1 GHz because the attenuation per unit length exceeds this frequency. As a result, to maintain the loss in the feeder cable, the diameters of the cables must be increased, significantly increasing the weight and cost of these cables [2]. In addition, there is a reasonable likelihood that the leaky feeder can be destroyed due to vehicle accidents and tunnel fires, which may cause the failure of wireless telecommunication data transmission. Therefore, a leaky feeder is typically not used in telecommunications to establish telecommunication networks within tunnels [3]. Understanding the flow mechanism of radio waves through the tunnel is essential to appropriately install transmitters and receivers to meet the system's requirements. The statistical properties of the wireless channel must be considered when determining the transmitter and receiver characteristics, and calculating the budget link. Various models have been proposed to determine these statistical properties. These models often forecast the path loss and power delay characteristics between a certain source and the terminal device wireless access point [4].

As previously stated, radio wave propagation inside the tunnel differs from other propagation environments such as in outside open air, outside confined establishments, or only inside confined establishments. The main difference is that the radio wave in the tunnel cannot reach the receiver directly because of the surrounding surface. Consequently, the transmission of radio signals within the tunnel must be managed differently from typical scenarios. Furthermore, tunnel structures vary widely in length, surface materials, moving objects inside the tunnel, surface roughness, electrical properties of objects inside the tunnel, antenna height, and tunnel shapes. These factors significantly affect the wave propagation model resulting in substantial diversity, making the propagation modeling more complex.

A comprehensive survey about propagation of waves in tunnels lacks in the literature, including the recent development of electromagnetic wave transmission in tunnels. The survey in [4] was conducted a few years ago; new literature has been added to the domain of expertise, making the survey outdated. In [5] and [6], different types of ray tracing methods for radio-wave propagation in tunnels were discussed. In Table 1, the main focus of all related existing surveys and their content, such as the classification employed, inclusion of intelligent models, and comparative studies, are discussed. Notably, some items in the survey were ignored or were not proposed in the literature during that time, as shown in Table 1. In [7], a survey of wave propagation models is presented but it is a generic survey containing most of the models related to the indoor environment. This study includes all the missing items, including the recent literature. Consequently, this study provides state-of-the-art knowledge on wave propagation inside tunnels.

In this study, wave propagation models for tunnels were analyzed in depth and evaluated qualitatively with regard to their notable features, characteristics, competitive

advantages, and limits. The primary contributions of this study are as follows:

- A complete and up-to-date analysis of the mechanism of wave transmission through tunnels is given.
- The models for wave propagation inside tunnels are sorted into groups based on their underlying approximation processes.
- The wave propagation models examined for tunnel interiors are qualitatively evaluated in terms of exceptional features, characteristics, competitive advantages, and limits. This comparison can help researchers and engineers choose, based on their needs, the wave propagation model that works best for them.
- Important unsolved research problems and the complications faced in developing wave propagation models are also discussed.

The remaining parts of the article are organized as follows. In the following section (Section II), we present a short overview of the fundamental factors associated with tunnel electromagnetic wave transmission techniques. In Section III, the wave propagation models for applications inside tunnels are evaluated thoroughly. The distinctive qualities, possible benefits, and drawbacks of the model are discussed. In Section IV, the wave propagation models for the interior of the tunnel are qualitatively examined with respect to their notable features, characteristics, competitive advantages, and limitations. In Section V, open research questions and problems related to the wave propagation models for tunnels are explored. The conclusion of this paper is presented in Section VI.

II. BACKGROUND

In this section, the essential aspects of issues related to wave propagation techniques inside tunnel are discussed, such as the geometric structure of the tunnel, regularity of the shape of the tunnel, objects inside the tunnel, and effects of the tunnel wall.

A. GEOMETRIC SHAPES OF TUNNEL

This section discusses the different reported geometric shapes of tunnels, as per the literature. We reviewed a wide range of tunnels in the literature to determine the wave propagation models. In [10] and [11], circular tunnels were discussed, where the tunnel environment was a subway. In [12], cylindrical tunnels were considered, and the study concentrated on the scattering of a plane wave. Radio communication in curved tunnels was discussed in [13], [14], and [15] analyzed electromagnetic wave transmission in arch-shaped tunnels for transportation operations. A discussion on arch-shaped rough wall tunnels is provided in [16]. Propagation in tunnels in which the tunnel shape is a *periodic jointed tunnel* was explained in [17]. Low-frequency propagation in idealistic rectangular-shaped tunnels was discussed in [1], [18], [19], and [20]. In [21], the propagation of radio waves was analyzed; the considered tunnels contained curved roads. Because the walls of the tunnels are not smooth in many

TABLE 1. Summary of existing related surveys. [C=classification, S=scaling-based, I=intelligent model, CA=computation advantage, CL=computational limitations, CS=comparative study].

| Ref. | Year | Description | C | S | I | CA | CL | CS |
|------|------|---|---|---|---|----|----|----|
| [4] | 2014 | The goal here is to develop an appropriate receiver that will receive and decode the sent signal, which has been corrupted because of the multipath and dispersion effects of the radio channel. Understanding the various propagation models can help to solve both challenges. Some of these approaches' benefits and drawbacks are summarized. | ✓ | ✗ | ✗ | ✓ | ✓ | ✗ |
| [8] | 2002 | An overview of current propagation prediction methods varies from early simple empirical formulae to advanced site-specific ray tracing-based models are discussed to meet the challenges of wave propagation model in new environments to pave the path for creating an integrated indoor or outdoor urban propagation model. | ✓ | ✗ | ✗ | ✓ | ✓ | ✗ |
| [9] | 2017 | In the survey, tunnel propagation path loss differs from channel characteristics to other high-speed trains (HST) scenarios. It shows some tunnel channel models created using various modeling techniques. | ✓ | ✗ | ✗ | ✓ | ✓ | ✗ |
| [7] | 2020 | This study extensively reviews radio wave propagation models for outdoor-to-indoor (O2I), indoor, and indoor-to-outdoor (I2O) applications. However, the tunnel propagation models are not extensively covered. | ✓ | ✗ | ✗ | ✗ | ✗ | ✗ |

cases, an additional amount of power loss is required to consider rough wall tunnels. In [22], such rigorous numerical modeling of wave transmission with a rough wall surface was considered. Because not all tunnels are straight or regular, the joining or cross-sections are different. A comprehensive statistical analysis of propagation in tunnels consisting of rough surface walls was performed in [23]. In [24], a discussion on different structural shapes and typologies is provided [1]. In [25], propagation modeling in complex utility tunnel environments, which considers different structural changes because of utility. In addition, in [26], it was shown how the existence of different objects (vehicles) inside the tunnel can affect the propagated wave. Geometric-based MIMO analytical channel model for vehicle communication was proposed in [27] and [28] to calculate important channel parameters such as power delay profile, and Doppler spectral density. These analytic studies may aid future vehicular communication channel development.

B. RELATED TOOLS

Some ready-to-use tools may be beneficial for locating transmitter and receiver sites to determine propagation characteristics, such as the power delay profile, propagation loss, multipath fading, and Doppler shift whereas installing telecommunication equipment within the tunnel. Under many circumstances, ready-to-use tools may be helpful for network management. A few of these tools are described in this section.

Tunnel visualization tool (TVT): It supports the following tunnel and radio parameters: conductivity, dielectric constant, antenna gains for transmission and reception, transmitted power, frequency, radio receiver sensitivity, and a path selected by the user [1].

Ray optics simulation: In order to use this virtual lab, the user must generate the necessary components, such as mirrors, lenses, and rays or beams. This virtual lab can conduct a wide range of optical geometry investigations. The virtual laboratory has been used to refract light, reflect light, and converge and diverge light from a mirror and lens [29].

Wireless Insite software: This software [30] has been used to simulate propagation scenarios with wave propagation parameters such as transmitting power and antenna height, and the results agreed with the measured results in [24].

Cloud-based ray tracing simulator (CloudRT): As a deterministic modeling tool, CloudRT simulations may provide complete information on multi-track effects in a variety of domains and generate realistic site-specific channel models. CloudRT simulations can also give a wide range of domain-specific information. It was implemented by Beijing Jiaotong University and the Technische Universität. It can track rays, such as direct, reflected, and scattered rays, using various means of propagation, and can make multiple measurements in the sub-6 GHz and terahertz (THz) band to verify and quantify the results of these tracking. In addition, users have the ability to construct their own channel in relation to the environment by rebuilding the 3D scenario model and setting simulation parameters (such as the frequency and antenna layout) [31], [32], [33], [34].

C. WAVE PROPAGATION TECHNIQUES

For tunnels, radio-wave propagation techniques are different from those for other non-confined spaces, as tunnel propagation models are limited by many internal reflections, refraction, and direct links. As a result, generally, the ray tracing technique, waveguide analysis, measurement-based empirical modeling, numerical modeling, and some hybrid techniques, which contain a combination of two techniques, such as (for example) numerical and ray tracing techniques, are employed.

III. TAXONOMY OF PROPAGATION TECHNIQUES IN TUNNEL

This section reviews the literature on the electromagnetic wave transmission mechanism inside tunnels. It develops a taxonomy of wave propagation, as shown in Fig. 1, that can be classified into three types: core, hybrid, and empirical model.

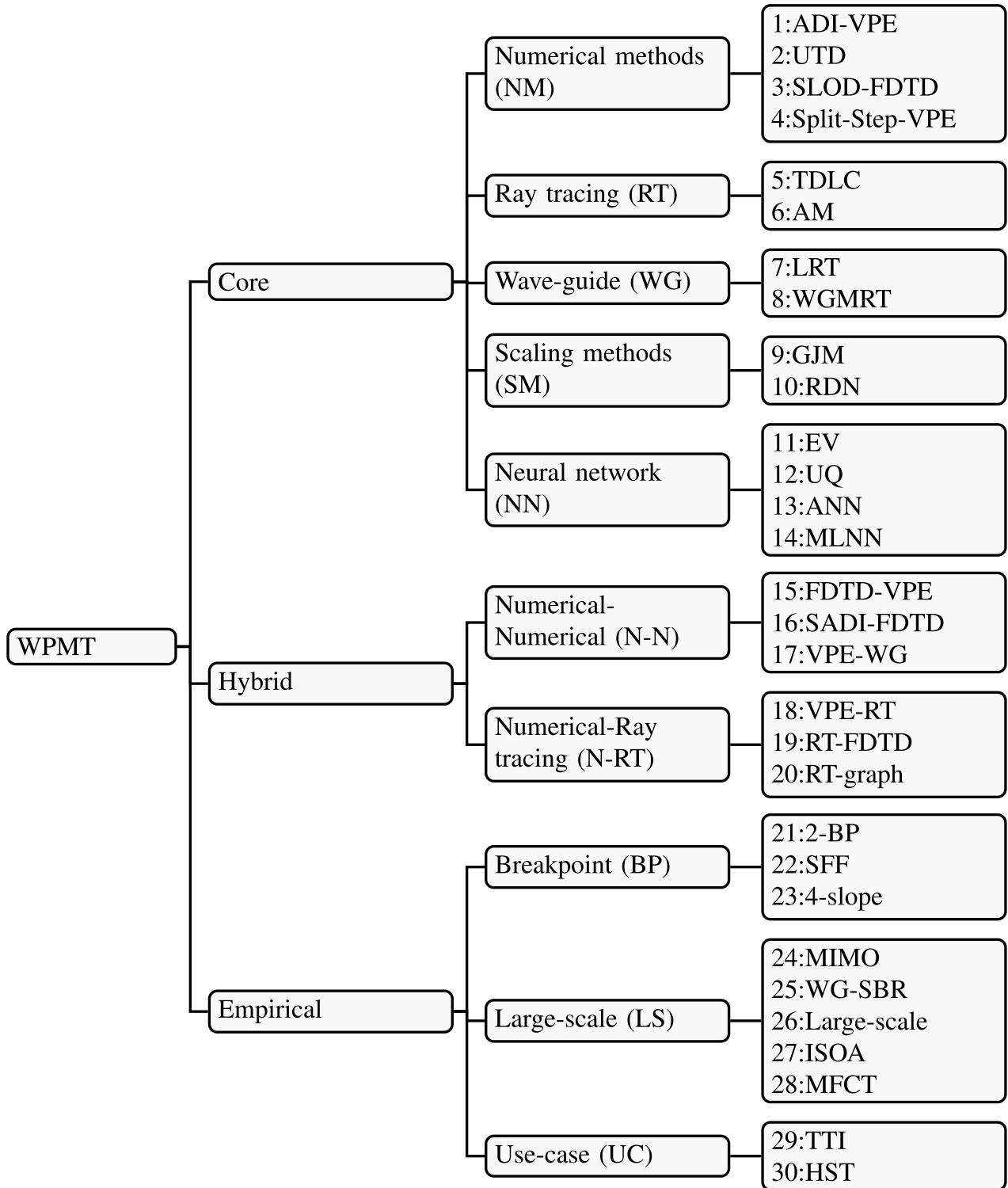


FIGURE 1. Taxonomy of wave propagation for the tunnels. Table 2 contains the abbreviations that are not included in this figure.

In the core model, wave propagation techniques are examined based on fundamental techniques that can be further classified as the numerical solution technique of Maxwell’s equation, ray tracing, waveguide, scaling, and recently emerged

neural network-based model. In certain instances, these standalone techniques cannot correctly represent the wave inside the tunnel; another type of model called a hybrid, composed of multiple primary techniques, has been proposed in the

TABLE 2. List of abbreviations.

| Abbr. | Elaboration |
|-----------|--|
| ADI | Alternate direction implicit |
| AM | Asymptotic methods (ray tracing) |
| BP | breakpoint |
| BW | Bandwidth |
| CFL | Courant-Friedrichs-Lewy |
| CloudRT | Cloud-based ray tracing simulator |
| CPML | Convolution perfectly matched layer |
| EV | Electromagnetic vision |
| FDTD | Finite-difference time-domain |
| GJM | Gerasimov, Jacob model |
| GTD | Geometrical theory of diffraction |
| HST | High speed train |
| ISOA | Improved seagull optimization algorithm |
| LRT | Lossy rectangular tunnel |
| LS | Large-scale |
| MFCT | Multi-frequency curved tunnel |
| MI | Machine learning and intelligence |
| MIMO | Multiple input and multiple output |
| MLNN | Multi-layer neural network |
| NM | Numerical methods |
| NN | Neural network |
| N-N | Numerical-Numerical |
| N-RT | Numerical-Ray tracing |
| POI | Point of interest |
| RDN | Ray-density normalization |
| RT | Ray tracing |
| SADI-FDTD | Segmentation ADI-FDTD |
| SFF | Slow/fast fading |
| SLOD-FDTD | Segmented locally one-dimensional FDTD |
| SM | Scaling methods |
| TDL | Tapped-Delay-Line |
| TDLC | Tapped-Delay-Line channel |
| TETRA | Terrestrial trunked radio |
| TTI | Train-to-infrastructure |
| TVT | Tunnel visualization tool |
| UC | Use-case |
| UHF | Ultrahigh frequency |
| UQ | Uncertainty quantification |
| UTD | Uniform theory of diffraction |
| VPE | Vector parabolic equation |
| WG | Waveguide |
| WGMRT | Wave-guide for metropolitan railway tunnel |
| WG-SBR | Waveguide-shooting and bouncing ray |
| WPMT | Wave propagation models for the tunnel |

literature. The empirical models mathematically interpret the overall characteristics of radio wave propagation and are based on measurement-based data. The empirical model can be further classified as breakpoint and use-case models. In the breakpoint model, multiple slopes are observed from the measurement data. The use-case models are based on specific application areas of wave propagation that consider different infrastructural elements and vehicle movement. All the models from the taxonomy are discussed in the next section.

IV. PROPAGATION MODELS IN TUNNELS

This section provides a detailed survey of the propagation techniques inside tunnels based on their essential

characteristics and differentiating aspects. A taxonomy based on the wave propagation models in the tunnel (WPMT) is first developed, and the models included in the taxonomy are discussed subsequently in terms of their principles, application specifications, advantages, and disadvantages.

A. CORE MODELS

Finite-difference time-domain (FDTD) is a well-known method for solving partial differential equations at a discrete time and distance, and that has been used in propagation techniques in tunnels. The solving procedure is done by dividing a space into grids and then determining the electric and magnetic field strengths of the grid in time and space. The problem with the FDTD method is that it needs a significant amount of computer processing power, which limits where it can be used for electromagnetic wave propagation in a tunnel when using a standard computer setup. The technique provides a software-implementable solution in the time domain. However, this only applies if the spatial grid is sufficiently precise to discern the model's shortest electromagnetic wavelength and the minor geometric features [4].

To reduce the computational difficulty, a hybrid FDTD approach comprising the ray tracing technique, which facilitates analysis of a wide area, and the FDTD, which was utilized to analyze regions adjacent to complicated discontinuities because ray tracing methods applied to regions with discontinuities generate extra complexities in such areas, was proposed in [35].

In [36], another type of hybrid technique that could be used to reduce computational complexity was proposed. This technique uses the vector parabolic equation (VPE) method for long distances and the FDTD method in areas with obstacles or antennas. Therefore, the model has a structure that is analogous to that of the FDTD-VPE-FDTD model. The FDTD method's amplitude value, as well as the time steps, are taken into consideration as the input of the VPE model. However, transferring the time steps to the frequency domain is necessary. Moreover, the VPE model imposes an additional constraint, which states that the propagation angle must be constrained to 30 degrees or less at all times. An in-depth error analysis is presented in [37].

Maxwell's equations are a set of correlated partial differential equations that form the foundation of electromagnetic theory. These partial differential equations can be put together to show how the electromagnetic field propagates at the speed of light. Maxwell's equations are approximated by parabolic equations under the assumption that most electromagnetic energy travels down a tunnel and that changes in the electric field along the tunnel are negligible compared to changes in the electric and magnetic fields that travel over the tunnel. Scalar parabolic equations are satisfied when the transverse electric and magnetic fields move in opposite directions, such as in a tunnel with conducting walls. In reality, tunnel walls do not conduct electricity efficiently; therefore, a relationship exists between the magnetic and electric forces. Using vector

parabolic equations in combination with the *Crank-Nicolson (CN)* method may effectively resolve this problem [4].

Subsequently, the parabolic equation-based tunnel propagation problem was satisfactorily modeled using the alternating direction implicit (ADI) technique [38], [39]. Whereas the ADI approach retains the same degree of accuracy as the CN system, it is much quicker and unconditionally stable in terms of cell size throughout the propagation path. Another change made by ADI itself may be corrected by utilizing an innovative technique devised by *Mitchell and Fairweather* in order to improve accuracy significantly [40].

1) NUMERICAL METHODS

The high-accuracy ADI technique for the vector parabolic equation is addressed in [41]. It has been suggested that the hybrid vector parabolic equation and waveguide mode theory should be used [16]. The hybrid vector parabolic equation was discussed in [42] as a method for modeling propagation in railway environments. In [43], a novel form of the ADI-VPE method with precision to the fourth order was presented for predicting the wireless transmission of electromagnetic waves in tunnels. Radio wave propagation in tunnels was predicted using a wide-angle three-dimensional ADI-VPE technique, as described in [44]. Numerical methods for solving the vector parabolic equation in a tunnel were discussed in [45]. In addition, [46] presented an alternative method for solving three-dimensional parabolic vector equations. In [47], a contrast between the vector parabolic equation and ray tracing solutions was shown. Modeling wave propagation in tunnels using the Noye–Hayman implicit finite difference approach was the focus of the research presented in [48], which presents an effective way to do so. To simplify the FDTD methodology, [49] suggested using a modified version termed the segmented-locally one-dimensional FDTD approach. The FDTD approach can be used to model regions that include obstructions or antennae, and the VPE technique can be used to represent hollow tunnels that extend for a larger distance [36].

a: ALTERNATE DIRECTION IMPLICIT-VECTOR PARABOLIC EQUATION (ADI-VPE)

The parabolic equation was utilized in [38] and [50] as part of a strategy known as the alternate direction implicit (ADI) approach to analyze the transmission of radio waves through tunnels. The equivalent surface impedance determines the electrical quality of the walls that conduct the electricity. Another acceptable scenario for employing a VPE is that of a tunnel with lossy walls. However, using the VPE makes modeling the boundary conditions very difficult. Because the boundary conditions of the ADI intermediate planes are equal to those of the real plane, the overall accuracy of the model is degraded. Furthermore, when ADI is used in tunnels with circular cross-sections, the process of breaking down lines one at a time becomes critical. Furthermore, the ADI-VPE was utilized to mimic actual tunnels to compare the experimental data with simulation outcomes. When lower-order

modes prevail over longer distances, the VPE model offers the most accurate estimates of electric fields in real tunnels.

Advantage: The VPE can predict low-order modes for electrically large tunnels with high accuracy [38], [50].

Disadvantage: The conventional VPE is an approximation of the *Helmholtz equation*, which makes the assumption that the fields move within 30° in the direction of propagation. The VPE makes a rapid adjustment to the numerical transform; however, this adjustment does not consider backscattered fields [39].

Application: The model is as efficient as the radius or complete wave methods, although arbitrary cross-sectional tunnels and soil height changes are considered [51].

b: UNIFORM THEORY OF DIFFRACTION (UTD)

In [52], diffraction by a right-angle wedge under various surface boundary conditions was calculated. A functional transformation was used to simplify the complexity of the boundary conditions. The incident field on the edge multiplied by the accompanying uniform impedance diffraction coefficient yielded a diffracted field. A surface wave may be derived from the common problem of a locally infinite surface when the impedance surface supports a surface wave. A wedge impedance model based on UTD was constructed to evaluate the propagation of ultrahigh-frequency (UHF) radio waves in tunnels [53], [54] that compared the experimentally measured path loss with the theoretical path loss. In an empty straight tube, the attenuation rates varied before and after the breakpoint. The propagation had a small delay spread and a broad coherent bandwidth under ideal conditions. Curved or branching tunnels limit coverage. In tunnels, transmission and reception are poor, as tunnel vehicles hinder propagation. The presence of a vehicle causes signal oscillations, losses, and RMS delay spread. Earlier tunnel propagation studies focused on narrow-band transmission rather than wide-band propagation. Frequency increases cause greater RMS delay spread, limiting the coherent channel bandwidth. These results match those obtained with the narrow-band tunnel simulations. The calculated and observed RMS delay spreads of the wideband multipath components are also similar.

Advantage: This model can predict the loss of radio coupling from a straight tunnel to a cross-section. The model was validated using measurements obtained from actual concrete tunnels. It can help optimize the deployment of wireless sensor nodes in underground mines [54].

Disadvantage: The model demonstrated simulated and measured received power for four frequencies with horizontal polarization for a junction crossed perpendicularly. Thus, this demonstration cannot be used for junctions where the tunnels do not cross perpendicularly.

Application: The UTD is an advanced approach used to resolve electromagnetic dispersion problems in more than one dimension at the same point by electrically tiny discontinuities.

c: SEGMENTED LOCALLY ONE DIMENSIONAL FINITE DIFFERENCE TIME DOMAIN (SLOD-FDTD)

In [49], a segmentation procedure was proposed to divide the one-dimensional FDTD processed signals of tunnel lengths. This procedure reduced the computational complexity of the FDTD method. The lengths of the segmented tunnels can be connected cumulatively.

Advantage: This model enhances the computation efficiency of the SLOD-FDTD technique by decomposing the computation space into smaller parts where a convolution perfectly matched layer (CPML) is then used to recombine the decomposed parts.

Disadvantage: It is not suitable for small-sized tunnels as they can generate smaller time step sizes that may not be used to overcome the stability condition of *Courant-Friedrichs-Lewy (CFL)* numbers. The CFL is a necessary condition that needs to be satisfied for convergence when numerically solving certain partial differential equations.

Application: The proposed segmentation technique can be applied to long-path propagation modeling to reduce the complexity of the FDTD technique.

d: SPLIT-STEP-VPE

In [55], an alternative method of FDTD called split-step Fourier transform (SSFS) is proposed to solve the vector parabolic equation, which can be expressed as (1):

$$u(x, y, z \pm \Delta z) = F^{-1} \{P(q_x)P(q_y)F\{u(x, y, z)\}\} \quad (1)$$

where F and F^{-1} are the Fourier transform pair; q_x and q_z are the spectral variables, and $P(q_\zeta)$ is given by (2).

$$P(k_\zeta) = e^{-jq_\zeta^2 \Delta z/2q_0} \quad (2)$$

where ζ is either x or y . The $+$ and $-$ symbols in (1) represent forward and backward propagating waves.

Advantage: It provides the application feasibility of the parabolic equation method through a split-step (vector) parabolic equation (SSPE) mechanism.

Disadvantage: The computed attenuation was not compared with other methods of computation-aiding mechanisms.

Application: The method showed promising performance in modeling radio wave propagation in a pedestrian tunnel environment.

2) RAY TRACING

The notion of rays is evident based on our daily experiences with sunlight. More strictly, a high-frequency approach to Maxwell's equations can describe ray notions. It is assumed that (i) a ray moves in a straight line in a homogeneous medium; (ii) a ray obeys the laws of reflection, refraction, and diffraction; and (iii) a ray carries energy. It makes more sense to think of a ray as a tube (that wraps around the central ray) in which energy is held and spread. Ray tracing can be used to show how transmitter-to-receiver techniques work and to find all of the possible ray paths between the

used point-to-point pairs [6]. In the ray tracing method, it is impossible to consider all the possible paths to the receiver, because the original transmitter-generated rays are reflected and diffracted before they reach the receiver. The problem worsens as the path length of the source ray increases, the wavefront side of the ray tube expands, and the object's size becomes less important. The ray model is useful when the antenna is small in comparison to the waveguide dimensions and runs at a frequency that is much higher than the cut-off for low-order modes. Note that the wavelength cut-off point for the lowest-order mode is [1]

$$\lambda < 2a \quad (3)$$

where the symbol a is the largest dimension of the tunnel cross-section. The ray model is particularly useful in situations in which the use of modal decomposition presents difficulties. According to [1], one of the advantages of the ray model is that it provides a natural approach for dealing with antenna layouts and tunnel junctions. However, with the ray model, extensive record-keeping is required to monitor all the essential reflections [1]. The ray can be classified into direct rays, reflected rays, diffracted rays, and scattered rays [56]. The ray tracing methods consist of ray generation, ray transmission, and ray reception techniques.

a: TAPPED-DELAY LINES (TDL)

TDL models need the best hardware requirements to be used in emulators [57]. The proposed model characterizes the power-delay profile (PDP), Doppler spectrum, and fading properties.

Advantage: This tunnel model includes the effect of the *rolling stock*, as the model is composed of snapshots of the tunnel environments, which include the number of rays, ray energy, and the delay of the ray.

Disadvantage: The time-domain analysis of TDL signals is very restricted if the smallest delay is smaller than 8 ns (in this case, it will require enormous bandwidth (BW); for instance, analysis of a 1 ns TDL will require a 1 GHz BW).

Application: With a minimum 8 ns time delay due to multipath fading, the TDL model combines the multipath with a minimum of 60 dB power of a ray.

b: ASYMPTOTIC METHODS (RAY TRACING) (AM)

Asymptotic methods such as ray tracing, ray launching, and tessellation of the tunnel arch section were used to construct an electromagnetic wave propagation model in [58]. This model was used to simulate the transmission of radio waves using data collected from straight arch-shaped tunnels. In addition, an interpolation technique for the normals of facets was developed to alleviate the inaccuracy generated by tessellation. The collected findings were validated by comparing them to those in relevant literature and measurement data.

Advantage: Asymptotic techniques, such as ray tracing and ray launch, are used to construct a model for transmitting radio waves via straight arch-shaped tunnels. It was

believed that interpolating the facets' normals would reduce the inaccuracy.

Disadvantage: It lacks adequate analytical analysis.

Application: This technique makes use of interpolation of the normals of facets in order to reduce the amount of inaccuracy that is caused by tessellation. This technique enables us to obtain findings using a convergent approach by considering a large number of different variables.

3) WAVE-GUIDE-BASED METHODS

There is a resemblance between the microwave waveguide and tunnel wall in terms of their shape and ability to conduct electromagnetic waves. However, the tunnel wall is not as conductive as a real waveguide, which results in the loss of the propagated wave. As a result, the tunnel can be treated as a microwave guide as long as it enables electromagnetic wave propagation. Otherwise, in the tunnel, modal mode propagation can not be considered, as the tunnel can violate the boundary condition. For example, for frequencies less than the cut of frequency f_{mn} inside the tunnel, where m and n are the TE and TM modes, respectively, the operating frequency decays and attenuates completely. Instead of the TE and TM modes, in tunnels, hybrid modes (HE) appear to be the normal modes, where the electric and magnetic fields need not be restricted to be confined within the traverse plane. Because modal theory understands the tunnel as a lossy waveguide with a regular cross-section structure, finding the Eigen function for the arch-shaped tunnel's cross-section is challenging [36]. In [59], modal methods were used to describe the electromagnetic wave transmission in lossy rectangular tunnels, and it was shown that, in the distant zone of an electrically large tunnel, both the modal and ray tracing techniques might be equal using the approximation (4):

$$E_r(x, y, z) = E_t \sum_{m=-\infty}^{+\infty} \sum_{n=-\infty}^{+\infty} \frac{e^{-jkr_{m,n}}}{r_{m,n}} \rho_{\perp}^{|m|} \rho_{\parallel}^{|n|} \approx \frac{-j2\pi E_t}{ab} \sum_{p=1}^{+\infty} \sum_{q=1}^{+\infty} A_{p,q} \frac{e^{-(\alpha_{p,q} + j\beta_{p,q})z}}{\beta_{p,q}} \quad (4)$$

where $E_r(x, y, z)$ is the electric field at point $R(x, y, z)$ within a rectangular waveguide that is obtained by summing the scalar electric fields of the rays from all the images of the point source, E_t is the magnitude of the transmitted electric field, k is the wavenumber in the waveguide, and $r_{m,n}$ is the distance between the receiver; ρ_{\perp} and ρ_{\parallel} are reflection coefficients corresponding to the perpendicular and parallel polarization, and the other symbols are indicated in Fig. 2.

The left side of (4) is the ray representation of the electric field and the right side represents the modal representation.

The multimode waveguide model provides an analytical equation for calculating the route loss and delay spread at any point in a tunnel [60]. This reveals that the attenuation mode is determined mainly by the diameter and operating frequency of the tunnel, whereas the distribution of power among the

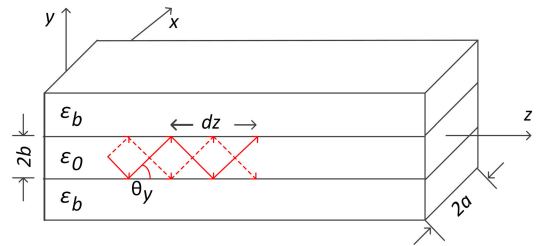


FIGURE 2. Geometry of the rectangular dielectric waveguide.

paths in various modes is determined by the location of the transmission antenna.

In [61], the modal analysis inside the tunnel was proposed. When the wall is assumed to be rough, the roughness should be within a certain limit such that it is smaller than the wavelength, as in equation (5), which was derived based on the assumption of a small roughness value.

$$\rho_s = \exp \left\{ -8 \left(\frac{\pi \sigma_h \cos \theta_{\perp, //}}{\lambda} \right)^2 \right\} \quad (5)$$

where ρ_s is an attenuation factor independent of the polarization status of the incident waves, σ_h is the roughness of the surface, and λ is the wavelength.

A unique simulation tool based on the modal transmission line matrix approach was specifically adapted to the context of tunnel wave propagation. Surface impedance boundary conditions were used to represent tunnel walls. The estimated modes for various tunnel cross-sections were then analyzed [62].

This technique is advantageous because it is proven and can immediately manage terminations and reflections [1].

The downside of modal decomposition in this application is that the transmitting and receiving antennas stimulate a wide range of modes. Additionally, tunnel junctions and other discontinuities introduce difficult-to-test mode interconnections. Modal decomposition can also involve a complex tunnel topology [1].

a: LOSSY RECTANGULAR TUNNEL (LRT)

Modal and ray tracing techniques are commonly utilized to simulate RF propagation in tunnels. Mathematically, the two procedures are equal and give the same outcomes. The comparative results of these two models with theoretical predictions from both techniques and field observations at frequencies of 455, 915, 2450, and 5800 MHz exhibited excellent agreement [59].

Advantage: This study analytically showed that the ray tracing method and the RT methods could show similar analytical behaviors under certain restrictions such as (i) the Tx and Rx are far enough, and (ii) the direction of the E-field remains almost unchanged after each reflection that leads to use as scalar summation.

Disadvantage: The RT and waveguide model exhibited similar performances under some specific conditions, such

as at a high frequency, in a long tunnel, and in a concrete structure tunnel. The equivalence behavior was not tested in other cases, and the limiting values of the frequency and length were not determined.

Application: Some standard configurations, like a square or circle for the cross-section of the wavelength, are used to study constants such as the cut-off frequency and wave impedance. This contribution can be helpful in the analysis of different types of tunnels, either through ray tracing or modal methods.

b: WAVEGUIDE FOR METROPOLITAN RAILWAY TUNNEL (WGMRT)

The millimeter-wave (mmWave) bands in urban railway tunnels were the subject of this study [63]. The findings of a propagation measurement effort in the 24 GHz band with a passenger aboard in a realistic subway environment were combined with ad hoc tunnel simulations and a theoretical modal propagation model. In receiving and transmitting antennas with horizontal and vertical polarization, narrow-band and wideband research has been conducted to estimate the link loss, fading, power-delay profile, and angle of arrival. This validation can be used to design and implement mmwave-based wideband mobile communication networks in train environments.

Advantage: The measured result and the simulated modal-based received power inside tunnels agreed on most of the length of observed tunnels.

Disadvantage: The path loss exponent values were not justified considering the tunnel environment.

Application: The results of this study inform the deployment of wireless communication links in the mmWave frequency band in a metropolitan tunnel.

4) SCALING-BASED METHODS

Reliable measurements in actual tunnels are challenging and costly to perform owing to instrumentation and access difficulties. Therefore, implementing scale-modeling methodologies for tunnels made of widely available materials may be a suitable option.

The scaling approach was theoretically validated in a waveguide with dielectric boundaries using image theory and in a perfectly conducting corrugated circular waveguide using the fast mode decomposition technique [64].

a: GERASIMOV, JACOB MODEL (GJM)

This investigation [65] uses of the ray tracing approach, which may be applied to structures with many orders of magnitude larger than the operational wavelength. Using image theory, the authors developed a multi-ray model to demonstrate non-dimensional properties. The multi-ray model helped to collect measurements in reduced trials. The results of a field experiment that was conducted in a small concrete pedestrian tunnel with smooth walls at 1, 2, 4, and 10 GHz, as well as in a scaled-down model utilizing millimeter waves (mmwave), revealed how frequency,

polarization, tunnel size, and dielectric properties affect wave propagation. Ray tracing was successful when applied to both the experimental data from the tunnel and a scaled-down model of the tunnel.

Advantage: This approach could be used to study the scaling property of a tunnel through a dimension of the tunnel. The validated results revealed that the wave propagation in a tunnel could be scaled down to study it at the laboratory level experimentally.

Disadvantage: Even though the predicted received power through the scaled mechanism follows the measured power, there is scope for improving the scaled model. The performance worsens when the operating frequency is close to the W-band, where the wavelength is approximately 3 mm.

Application: It can be helpful to perform practical wave propagation modeling. In [64], a novel method for ray tracing using geometrical optics (GO) is presented. This method differs from the traditional ray tracing method in that it can create measured data in a lab setting that is identical to the measured data in an actual tunnel.

b: RAY-DENSITY NORMALIZATION (RDN)

RDN is a single ray representing a locally flat wavefront, and this novel approach requires several representations of each actual electromagnetic wave (EM) wave [64]. The proposed RDN specifies the contribution of each ray to the overall receiver field. The inability to play caustics is one of the most important disadvantages of GO, which is eliminated by this procedure. Unlike conventional methods, this unique technique does not use ray tubes or adaptive reception spheres. Therefore, the limits on the planar geometries do not affect them. Consequently, high-frequency EM wave propagation can be accurately predicted in enclosed tunnels.

Advantage: The method requires several representatives of every physical EM wave simultaneously. The contribution of each ray to the total area of the receiver is based on the RDN. As a result, it does not suffer from planar geometry limits. In addition, it allows the spread of high-frequency electromagnetic waves in confined places with curved limits, such as tunnels, to be predicted with appropriate precision.

Disadvantage: The assumption that, in a confined place, all rays will be reflected with the same group velocity and delay profile may not be valid for a tunnel with a rough surface.

Application: The use of normalization was shown to be effective for RT modeling in arch-shaped tunnels in [58]. Here, the same normalization technique is used to model the RT for scaling wave propagation in a tunnel.

5) NEURAL NETWORK

In recent years, AI and deep learning algorithms have demonstrated superior performance in different prediction systems consisting of adequate datasets. Typically, machine learning algorithms are used in nonphysical systems to study their behavior and yield a specific output. However, in recent years, it has been noted that these types of algorithms have been used in physical systems and, more specifically, for

modeling propagation waves. In [66], the authors propose a machine learning method for extracting radio wave propagation models in tunnels. They offer a framework for an artificial neural network, a suitable generalization of different geometries. The intended output might be the values of the electromagnetic field components throughout the channel or the path loss model.

a: ELECTROMAGNETIC VISION (EV)

In [67], the path loss inside a tunnel was proposed through the robustness of physics-based methods and real-time channel models usable by wireless networks through machine learning and intelligence (MI) using tunnel geometric information and the parameters generated through synthetic means either through VPE or ray tracing techniques. The path loss exponent (n) predicted by deploying the developed MI model demonstrates a high degree of agreement between the model predictions, actual measurements, and computer simulations.

Advantage: Machine intelligence models can be trained using ray tracing or parabolic equation methods to finally create an “electronic vision” to supply channel propagation based on a picture or sequence with the geometric specifications of the channel. Subsequently, using this vision, the path loss exponent of the tunnel was determined and showed satisfactory performance.

Disadvantage: The demonstrated scenario was simple in shape (rectangular tunnel) and showed a higher prediction error near the transmitter.

Application: The intelligent model feeds the scalar functions with the maximum and minimum values of the tunnel width, height, frequency, and permittivity to a three-layer artificial neural network, which can develop the path loss estimation. The sum-of-squares difference between the predicted path loss and the measured path loss model is the loss function that must be reduced to achieve the overall loss. Because the mechanism works for predicting path loss, it paves the way for deploying artificial neural networks to model path loss inside tunnels.

b: UNCERTAINTY QUANTIFICATION (UQ)

In [68], the VPE technique was used to generate a reasonable number of configuration parameters for wave propagation in a tunnel. The parameters generated by the VPE method showed nonzero standard deviation, which means that there is variance in the input dataset generated through such means. Therefore, an artificial neural network (ANN) was proposed to reduce such inconsistencies in the data used to develop a realistic wave propagation model inside a tunnel.

Advantage: The results reveal that, with a sufficient number of input datasets, the uncertainty of fidelity measured data can be solved by applying this technique.

Disadvantage: The presented results were obtained at a frequency less than 1 GHz, showing that a further test is required at a higher frequency.

Application: A deep ANN was utilized to evaluate uncertainty in VPE-based channel propagation model input

parameters. The ANN, which had six layers, was trained using a variety of input combinations, and a VPE-based process was used to create the input dataset.

c: ARTIFICIAL NEURAL NETWORK (ANN)

In [66], the ML-based wave propagation model inside the tunnel comprised several parts: a set of input parameters, the ML model, and the desired output. The input model comprised several microwave-link-based parameters, such as the transmitter and receiver specifications, antenna pattern, tunnel geometry, operated frequency bands, and wall materials. An extended part of the physics-based solver was responsible for determining all the parameters related to the physics that was supposed to follow. It connected all the input parameters to the input model to generate a dataset that fed the ML model (x) and parameter model (\tilde{x}). The feeding parameters generated through such means are significant because if a particular parameter can be neglected in the ML model, it can be necessary for the parameter model. Finally, the parameters x and \tilde{x} were used to train the ML model to determine the desired power level at the receiver end.

Advantage: This model has found some possible major problems with the application of ANN for tunnel wave propagation modeling: input, output, and ML model specification. The demonstrated results reveal that the ANN model outperforms the VPE model in terms of accuracy, scalability, and interpretation of the “physical rule.”

Disadvantage: The accuracy of this approach is close to that of the VPE method; however, according to the graphs in [66], it is evident that the predicted propagation signal power does not match well with the measured power.

Application: A comparison of the ANN data and both the VPE-generated and measured data revealed that the inference capabilities of the ANN model for unknown tunnel geometries were solid. Furthermore, the network’s scalability was excellent, allowing the ANN to maintain its precision, even when the number of input features increased.

d: MULTI-LAYER NEURAL NETWORK (MLNN)

The model is [69] considered nine input variables to predict the path loss, root square mean of the delay, and angle spread. The k-hidden layered backpropagation algorithm initializes with initial weights, initial biases of the neurons, and expected error rate. The hyperbolic activation function was used as the activation function in the neural network. The path loss was considered as $P_t - \sum_{l=1}^L p_l$, where P_t is transmitted power and P_l is received power of the l-th path. The RMS is an important second-order statistic to describe channel dispersion in the delay domain; it is calculated as $\sqrt{(\sum_{l=1}^L t_l^2 p_l / \sum_{l=1}^L p_l - \bar{t}^2)}$, where t_l is the delay of the l-th multipath. \bar{t} is the average additional delay, which can be defined as $\sqrt{(\sum_{l=1}^N p_l (\theta_l - \bar{\theta})^2 / \sum_{l=1}^L p_l)}$, where θ_l is the arrival angle of the l-th multipath. $\bar{\theta}$ is the average arrival angle, which can be defined as $\sum_{l=1}^N p_l \theta_l / \sum_{l=1}^L p_l$.

Advantage: This multi-layer neural network can predict large-scale and small-scale fading in metro tunnels.

Disadvantage: The training data set needs to be carefully collected as the relationship among the parameters is comparatively complex, and the change in one parameter can affect the change in other parameter output [16], [60], [70], [71], [72].

Application: The proposed technique can be applied to a metropolitan train tunnel environment to predict the path loss, root square mean of the delay spread, and angle spread.

B. HYBRID MODELS

Various techniques have been used to represent propagation channels in tunnel settings. Each method has its own benefits and drawbacks. Hybrid channel modeling methods have been investigated to obtain complementary benefits.

1) NUMERICAL-NUMERICAL

The FDTD method and VPE method were integrated in [36] to benefit from an analysis technique that reflects the real propagation mechanism. In this hybrid technique, the FDTD method is applied to the transmitter end and in spaces where there are more obstacles in propagating the radio wave. However, in the vacant part, the ADI variable of the VPE method is applied, and both methods are combined at a particular interface point that needs to be fixed appropriately.

a: FINITE-DIFFERENCE TIME-DOMAIN-VECTOR PARABOLIC EQUATION (FDTD-VPE)

A hybrid FDTD/vector parabolic equation (VPE) approach was presented in this paper [36] to explain the propagation of radio waves within rectangular tunnels. Whereas the FDTD technique is used to model regions, including barriers or antennae, the VPE method is used to represent long empty tunnels. The benefits of the two techniques may be used to improve the numerical efficiency of the investigation and evaluate the influence of the antennas. The results of the comprehensive FDTD simulation, as well as the measurement data collected in a corridor, were compared with the outcome of the hybrid strategy that was used. This method works well for simulating the propagation of radio waves via tunnels that contain antenna relays and other obstructions.

Advantage: In this hybrid method, the advantages of the FDTD method are deployed in areas with obstacles or antennas, whereas the easy computational benefits of the VPE method are deployed to model the empty tunnels along with the distance. This is a hybrid technique that is effective in tunnels with antenna relays and obstacles.

Disadvantage: Instead of a real tunnel, a typical indoor corridor was used in the experiment, which is a very strong limitation of this technique.

Application: The starting region for VPE is calculated based on the FDTD result, and the data are separated. The FDTD employs amplitudes and time steps to represent the interface field.

b: SEGMENTED ALTERNATING DIRECTION IMPLICIT FINITE DIFFERENCE TIME DOMAIN (SADI-FDTD)

For wave propagation within a long tunnel, this study [73] proposed a unique SADI-FDTD method. The proposed method lowers computational redundancy by segmenting the problem space. It also enables the use of larger cells in each section. The approach was tested by simulating the propagation in real tunnels and comparing the results with the existing experimental data. Comparisons revealed that the proposed method predicts the fields most accurately in long-distance tunnels.

Advantage: By segmenting the problem space, the proposed S-ADI-FDTD approach that was presented may reduce the amount of unnecessary computational work. It also makes it possible to use cells of a bigger size in each section.

Disadvantage: This method's applicability has not been tested for curved and branching tunnels with rough wall surfaces.

Application: The SADI-FDTD method does not offer any mechanism to improve the prediction ability of the propagated wave in the tunnel; rather, it just provides a mechanism that permits the central processing unit (CPU) to execute time linearly, whereas the convention ADI-FDTD exhibits exponential behavior in this case.

c: VECTOR PARABOLIC EQUATION-WAVEGUIDE (VPE-WG)

In this study, [16] combined the vector parabolic equation (VPE) with waveguide mode theory to simulate propagation accurately and efficiently. The VPE method analyzes propagation near the transmitter, allowing fast analytical field calculations across long distances using VPE fields. This hybrid model considers the tunnel geometry and antenna radiation patterns while reducing computing costs. A comparison of the measurements and simulation models for road and subway tunnels revealed the precision and efficiency of the proposed hybrid model.

Advantage: The use of VPE to estimate the dimensions of the rectangular waveguide that is utilized in this approach enhances its durability and adaptability with regard to the geometry of the tunnel.

Disadvantage: The overall execution time is reduced, but the mean absolute error (MAE) does not improve significantly.

Application: The performance of this method has not been verified at frequencies higher than 2 GHz.

2) NUMERICAL-RAY TRACING

Ray tracing model provides reliable means of wave propagation modeling in many studies [56], [74]. However, due to the huge complexity, this technique suffer from some disadvantages and huge computation problems [75]. However, the use of numerical techniques with the ray tracing methods can solve the complexity of computation issues and thus can help to develop a well-performing wave propagation model.

a: VECTOR PARABOLIC EQUATION-RAY TRACING (VPE-RT)

This paper provides a hybrid channel modeling approach that combines ray tracing with vector parabolic equation modeling [42], [76]. VPE advantages are utilized to compensate for RT restrictions and vice versa. The proposed technique allows for the modeling of realistic railway conditions within a single simulation framework. Stations and long guideway tunnels are two examples of such situations. An accurate deployment location for communication-based train control systems is selected to confirm these findings.

Advantage: This technique reduces the complexity of RT by using VPE.

Disadvantage: The drawback of this technique is that no definite rules are specified for the interface grid to combine the RT and the VPE.

Application: The vector parabolic equation is used for lengthy tunnel sections that are reasonably uniform, whereas ray tracing method is utilized for regions that have complicated geometries and discontinuities. In this model, the interface space between the RT and VPE is represented by the *Huygens surface*. This surface aids in the prediction and explanation of the classical wave propagation of light [77].

b: RAY TRACING-FINITE-DIFFERENCE TIME-DOMAIN (RT-FDTD)

In [35], ray tracing was used to analyze a wide area that was realized by using the *virtual box*, in which the RT mechanism of wave propagation is assumed to follow, and the FDTD was used to study areas close to complex discontinuities where ray-based solutions are not sufficiently accurate. This hybrid technique ensures improved accuracy and practicality in terms of computational resources.

Advantage: Ray tracing is used to analyze a wide area that is realized by using the “virtual box”, inside which the RT mechanism of wave propagation is assumed, and the FDTD is used to examine regions around complicated discontinuities when ray-based solutions are insufficiently precise. This hybrid method guarantees increased precision and computing resource practicability.

Disadvantage: The consideration of the *virtual box* makes it too difficult to apply this approach to a general case. This is because, in this model, the *virtual box* needs to be used where any *discontinuity* type surface exists.

c: RAY TRACING (RT)-GRAPH

Hybrid mmWave propagation by integrating the ray tracing and propagation graph theory inside metro environments was presented in this study [78]. By monitoring channels at 26.5-40 GHz and adjusting the parameters of the ray tracing models, electromagnetic wave propagation principles, object interactions, and specularly reflected rays are identified. This mmWave propagation model with scattered locations around RT's major RT pathways is presented to simulate diffuse scattering. The received power levels at different locations validated the proposed hybrid propagation mechanism. The

hybrid model is ideal for simulating multipath propagation in a closed metro train scenario, where multiple objects exist in close locations and the echo is a normal phenomenon.

Advantage: In this technique, ray tracing and graph theory are combined to consider the scattered points around the principal paths vigorously representing the diffuse scattering components.

Application: According to the findings, significant reflected elements are determined, and a maximum of two reflection hops are acceptable for RT capture of primary multipath components (MPCs). Two to eleven times as much power comes from diffuse components such as specular components.

C. EMPIRICAL METHODS

The empirical models are based on experimental data observations interpreted into mathematical relationships [79]. This type of model normally have some coefficient that are varied according to the tunnel type, tunnel shape, internal structure and operational frequency bands [70], [80], [81], [82]. Due to curvature structure in the tunnel there normally happens breakpoints [15], and the number of breakpoints also varies [83].

1) BREAKPOINT

In [84], it was observed that a single-slope regression fit yielded a much higher standard deviation.

It was found that the RT model can yield good propagation estimations in the near field, whereas the waveguide model is suitable for the far field. Thus, to take advantage of this, in [85], an analytical ray optical (waveguide) model was proposed, which is a tunnel propagation model where both of these RT and waveguide models can be used before and after a point called the breakpoint. In [59], it was shown that the RT and waveguide models exhibit equivalent behavior in rectangles, which can be extended to other regular-shaped tunnels.

In [15], the experimental results of radio wave propagation in a straight arch-shaped tunnel were presented. The results were compared with simulation findings obtained using the ray-launching technique applied to the tunnel. Two frequencies were used: 2.4 and 5.8 GHz. The rapid fading distribution fit the *Weibull distribution* for both observations and simulations.

a: 2-BREAKPOINT (BP)

Wireless propagation in a tunnel has discrete near-and-distant zones with diverse propagation characteristics. In [85] a 2-point break technique was used to split the propagation areas to determine propagation losses according to (6).

$$PL_n[\text{dB}] = PL_f[\text{dB}] \quad (6)$$

where PL_n and PL_f respectively denote the path loss developed by the analytical ray tracing model and single ray optical model. The analysis demonstrates that the location of

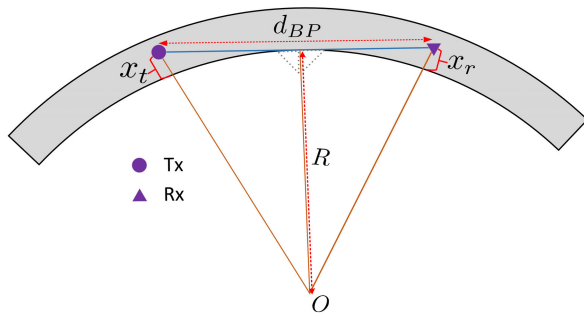


FIGURE 3. Graphical representation of the location for breakpoint [86].

the breakpoint is significantly influenced by the frequency, antenna position, and tunnel transversal dimensions. However, in [86], a different approach is proposed for a curved tunnel. In this approach, the breakpoint is defined on the radius of curvature of the tunnel as shown in Fig. 3, where the breakpoint was determined by (7).

$$d_{BP} = \sqrt{(R + x_r)^2 - R^2} \quad (7)$$

where R is the radius of curvature, and x_r is the distance indicated in the Fig. 3.

Advantage: The model offers an analytical approach for finding the breakpoint, which helps in the deployment of RT and the waveguide model in the tunnel.

Disadvantage: The model needs further improvements as the measurements and the slope-based resulted signal did not match accurately.

Application: The model is helpful in finding the breakpoint in a curvature tunnel, where the antenna gain does not affect the breakpoint.

b: SLOW/FAST FADING (SFF)

In [15], the slow and fast fading effects of wave propagation inside a tunnel were investigated, and the results were validated through measured datasets in arched cross-sectional straight tunnels using tessellation in multiple facets. The analysis was based on a ray tracing-based imaging technique, and it was shown that the number of facets varied with the operating frequency and tunnel dimensions.

Advantage: When the arch is represented by planar facets, the ray launching technique may be paired with interpolation of the facets' normal, resulting in an effective way of describing electromagnetic wave transmission in straight arch-shaped tunnels.

Disadvantage: The model used a modified ray launching model where the facets approximated the arch-shaped tunnel, and a method of interpolation of the facets' normal was implemented by the *Phong algorithm* [87]. However, they did not include a detailed mathematical analysis.

Application: This model, which is mainly based on the modification of the deployed RT model by the "identification of multiple rays" at the receiver (Rx) end, can be used in rectangular or arch-shaped communication tunnels.

c: 4-SLOPE

It offers [83] a path loss model with four parts based on field measurements: the high path loss segment, the Fresnel zone area, the waveguide segment, and the most distant area. The division points of the segments were described analytically. Propagation in free space is typical near antennas. Only a large percentage of the reflected rays from the near area reach the receiver in the following region, resulting in significant path loss. In distant areas, the waveguide effect is caused by a group of waves that are reflected off the tunnel walls, resulting in decreased path loss. Owing to the attenuation of the reflected photons in a very distant area, the waveguide effect was eliminated.

Advantage: The model can be applied to long tunnels depending on the carrier frequency, obstacles in the tunnel, and the transmitter, and or receiver position.

Disadvantage: The proposed model was based on a heuristic approach, and it has not been analyzed with the established theories of wave propagation, such as the waveguide propagation theory, ray optical models, and Maxwell's equations.

Application: Applicable inside road and railway tunnels where the operating frequency is 400 MHz using the EU standard-based Terrestrial trunked radio (TETRA). This study examined radio propagation in road and railway tunnels at 400 MHz in a 2 km tunnel. In the vicinity of an antenna, free-space propagation is standard. In the subsequent region, only a few scattered rays reach the receiver, resulting in high path loss. The channel route loss is divided into four parts by three breakpoints for a straight road tunnel: a space loss region, close area, distant area, and extremely far area. This four-slope path-loss channel model can be used to quickly predict the direct mode coverage in TETRA systems. The wave-guide effect disappears in the extremely far region owing to the attenuation of the reflected rays.

2) LARGE-SCALE MODELS (LS)

Wave propagation models consider detailed propagation phenomena such as reflection, refraction, absorption in the wall, and surface smoothness. Instead, the LS model considers the overall behavior of propagated waves and results on some statistical parameter [88] depending on the structure of the tunnel, obstacle probability, and operating frequency factors.

a: MULTIPLE INPUT AND MULTIPLE OUTPUT (MIMO)

In [89] the authors analyzed 32×64 massive MIMO radio channel and mathematical expression of power delay profile, path loss, angular spread, inter-user spatial correlation, and capacity. This research outcome can help analyze the huge antenna-based measured data in tunnel environment for yielding huge capacity to deploy machine-to-machine communication or other purposes.

Advantage: It adds spatial information to the models of 5G massive MIMO systems and suggests ways to improve the accuracy of mobile networks underground.

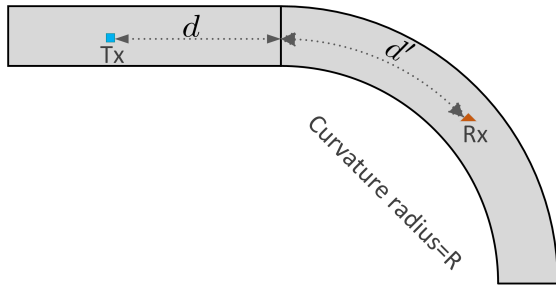


FIGURE 4. Cascaded straight and curved tunnel and Tx and Rx locations. All the distance units are in m [90].

Disadvantage: No mechanism was added to mitigate the near-end and the far-end disparity.

Application: This contribution extensively analyzes the measured path loss in the tunnel with the MIMO system.

b: WAVEGUIDE-SHOOTING AND BOUNCING RAYS (WG-SBR)

When the waveguide mode theory and the method of shooting and bouncing rays (SBR) are used together, it is found that both straight and curved tunnels lose power in the far-field region when they are stacked together. So, the authors came up with a method that takes an extra loss coefficient into account in the propagation model [90].

$$L_{total}(d + d') = L(d + d') + ELC(R) \times d' \geq d_{BP} \quad (8)$$

where d_{BP} is the breakpoint that can be determined using (9), and extra loss coefficient (ELC) can be determined using (10). The symbols d and d' are illustrated in Fig. 4.

$$d_{BP} = \max\left(\sqrt{\frac{2s}{1+\cos\theta}[(\pi-\theta)r^2+h^2\tan\theta]^2}/\lambda, \sqrt{\frac{s(1+\cos\theta)}{2}[(\pi-\theta)r^2+h^2\tan\theta]^2}/\lambda\right) \quad (9)$$

where r is the radius of tunnel, h is the distance from center to bottom of the tunnel, s and θ denotes the cross-sectional area ratio of a rectangular to a circular area.

$$ELC = 20K_s \log|\Gamma_s| + 20K_c \left(\log|\epsilon_r^* - 1| - (2\ln(-\sqrt{\epsilon_r^* - 1})/\ln 10) \right) + 20K_c \times \sum_{i=1}^N y_i / \ln 10 \times N \times \sqrt{\epsilon_r^* - 1} \times R^{-1} \quad (10)$$

where Γ_s denotes the reflection coefficients along the vertical walls in the section of straight tunnels, and The letters K_s and K_c stand for the number of reflections per meter in the straight and curved tunnel walls. It is assumed that the fundamental mode is reflected N times on the vertical wall of the curved tunnel with a length of d' .

Advantage: It is asserted that the suggested model has low complexity and can accurately predict path loss in cascaded train tunnels.

Disadvantage: The model requires comparatively complex 3D-RT techniques, which is comparatively complicated.

Application: They found the excess loss in the far-field region, which has a linear function of the path length of the tunnel curvature section.

c: LARGE-SCALE MODELS

In the literature, many large-scale models are proposed to model the measured path loss using empirical formulae such as Close-In (CI), Floating intercept (FI), CI model with a frequency-weighted path loss exponent (CIF), and alpha-beta-gamma (ABG) models [3]. Equations (11), (12) are the models used for single-frequency operation whereas (13), (14) are the models for the multi-frequency operation.

$$L(f, d)|_{CI} = F(f) + 10n \log_{10}(d) + X_\sigma|_{CI} \quad (11)$$

$$L(d)|_{FI} = \alpha + 10 \cdot \beta \log_{10}(d) + X_\sigma|_{FI} \quad (12)$$

$$L(f, d)|_{CIF} = F(f) + n \left(1 - n + \frac{bf}{f_0} \right) 10 \cdot \log(d) + X_\sigma|_{CIF} \quad (13)$$

$$L(f, d)|_{ABG} = 10\alpha \log_{10}(d) + \beta + 10\gamma \log_{10}(f) + X_\sigma|_{ABG} \quad (14)$$

where L denotes the path loss, F is the free space path loss with reference distance is 1 m, n is the path loss exponent, α is the floating-intercept in dB and this parameter is equivalent to free space path loss, and β is the slope of the line, b is the optimization parameter that presents the path loss slope of the linear frequency dependence, f_c is the center frequency $F(\text{dB}) = 32.4 + 20 \log f_c(\text{GHz})$, $f(\text{GHz})$ is the operating carrier frequency and f_0 is the minimum investigated frequency of operating frequencies.

In [91] and [92], it was that from a viaduct to a tunnel, the path loss exponent varies in different sections, which can be defined along the distance in the CI and AB models.

Advantage: This study gives the propagation parameters in HST environment.

Disadvantage: The effect of passengers on the train was not considered.

Application: It finds out that the statistical propagation parameters vary in rural, viaducts, or straight sections.

d: IMPROVED SEAGULL OPTIMIZATION ALGORITHM (ISOA)

In this technique [93] the standard propagation models (SPM) are enhanced by deploying the ISOA algorithm. RT propagation mechanisms were used to develop the basis of this technique. The position of the light wave was determined using helix radius r as in (15).

$$\begin{cases} x' = R \times \cos(\theta) \\ y' = R \times \sin(\theta) \\ z' = R \times \theta \\ R = u_x \times e^{\theta v_y} \end{cases} \quad (15)$$

where u_x , v_y are the parameters used to determine the helix shape, and θ is the random angle between $[0, 2\pi]$.

Finally, the ISOA updated the position according to (16).

$$\vec{P}_s(t) = \left(\vec{D}_s \times x \times y \times z \right) + \vec{P}_{best}(t) \quad (16)$$

where $\vec{P}_s(t)$ is the position of the population after an iteration, \vec{D}_s is the best search agent in the direction of convergence, and $\vec{P}_{best}(t)$ indicates the best position of seagulls.

TABLE 3. Innovative features of existing wave propagation models in tunnels.

| Ref. | Innovative features |
|-----------|---|
| EV [67] | The machine learning model determines the path loss exponent (PLE) in rectangular tunnels and proves that model predictions match actual and simulated data well. Techniques based on classical mechanics-based analysis, such as ray tracing and the parabolic equation approach, can train artificial intelligence models. |
| UQ [68] | The measurement-based propagation estimation model suffers from the variations in data and parameters that affect the estimation. Thus to remove such uncertainty, the machine learning-based propagation technique can estimate the received signal, which can be close to the measured signal strength. |
| ANN [66] | The tunnel structure dramatically influences the determination of the received signal strength. As a result, to deploy the ANN model to predict the signal strength at the receiver end, many parameters need to be selected. Compared to both the VPE-generated and measured data, the ANN-based model can determine the inference with the new tunnel geometry was strong. The additional benefit of the ANN-based technique is that the model is not excessively susceptible to any specific input parameters. |
| MLNN [69] | In the tunnel, wave propagation is influenced by many factors such as antenna position, signal frequency bands, propagation distance, and tunnel dimensions. Considering 3D distance additional three factors—x-coordinate, y-coordinate, and z-coordinate need to consider for Tx and Rx positions as well. In this study additional parameter, the radius of the arched tunnel was considered to predict the path loss, delay spread, and angular spread. The height of the antenna, type of antenna, and tunnel wall roughness can affect the path loss, delay spread, and angular spread factors. This study can be helpful for considering additional parameters that may have an effect on the wave propagation in a tunnel in the multi-layer neural network to determine different output parameters in the tunnel environment. |

The ISOA technique employs a random location equation to maximize the global optimization and periodic disturbance to avoid any possible premature convergence and enhancement of convergence speed.

Advantage: This model showed better performance than the simple standard propagation model. In addition, it can mitigate the unwanted disparity waveguide effect at the far end and the near end.

Disadvantage: The technique is tested at a frequency of 1.8 GHz. Therefore, to support a 5G network, it needs to test in the mmWave band. In addition to the ISOA algorithm described but how to relate the algorithm related variables to the wave propagation inside tunnel are not presented well.

Application: The model can correct several parameters of the RT propagation mechanism.

e: MULTI-FREQUENCY CURVED TUNNEL (MFCT)

In [71] it was established that the path loss exponent (n) of large-scale models could be accurately presented as (17).

$$n = c_1 + c_2d + c_3d^2 + c_4d^3 + c_5d^4 + c_6d^5 + c_7 \ln f + c_8(\ln f)^2 + c_9(\ln f)^3 + c_{10}(\ln f)^4 + c_{11}(\ln f)^5 \quad (17)$$

where d and f represent arc heights and frequency, respectively. $c_1, c_2, c_3, \dots, c_{11}$ represent different coefficients.

In this study, it was found that the root-mean-square (RMS) of the delay spread (DS) can be expressed as (18).

$$DS = -0.004(R - \sqrt{R^2 - 40000}) - 8.446; \text{ for } (R \geq 200) \quad (18)$$

where R is the radius of the curvature in m, and DS is the delay spread in ns.

Advantage: Multi-frequency supporting capacity and defining the path loss in terms of the delay spread, frequency, and tunnel curvature.

Disadvantage: There may be additional parameters that can affect the path loss, but those were not considered in the proposal.

Application: This neural network-based network can help design future-generation V2V channels.

3) USE-CASE (UC)

Tunnels have several applications, particularly in transportation. Each day, the train's speed surpasses its previous best, which impedes the appropriate modeling of wave propagation. This section examines some current literature on propagation modeling, particularly regarding high-speed or train-to-infrastructure communication.

a: TRAIN-TO-INFRASTRUCTURE (TTI)

Modern subway stations and their entry tunnels were investigated in [94] to describe wireless channels. The train maintained a consistent speed of 18 km/h from the tunnel entry point to the point at which it exited the station. The wireless channel response for both connections was characterized by multipath space-alternating generalized expectation-maximization (SAGE) using the parameter delay profile, root mean square delay spread, Doppler power spectral density, small-scale fading distribution, and K-factor.

Advantage: This experiment uses the transmitter and receiver to demonstrate the train-to-infrastructure communication while the train is on the move.

TABLE 4. Advantages and limitations of different propagation models.

| Ref. | Class | Advantages | Disadvantages | Remarks |
|-----------------------------|-------|--|---|---|
| 1 ADI-VPE [38] | Core | The VPE can simulate low order modes for electrically massive tunnels with precision [38]. | The VPE is an approximation of the <i>Helmholtz equation</i> based on the assumption that fields move within 30° toward propagation. The drawback of this method is that it responds quickly to numerical transform, which disregards backscattered fields. The VPE quickly adjusts to numerical transform, and that does not take account of the back-scattered fields [39]. | cross-section shape, wall impedance, slowly varying curvature, and torsion of the tunnel axis, two polarization are decoupled (for rectangular cross-section). |
| 2 UTD [52, 53, 54] | NM | UTD was developed to solve the problem of determining the amount of diffraction at the <i>shadow boundaries</i> as there exist discontinuities in the boundary. | (1) The object under analysis using the UTD method should be electrically large in terms of wavelength. (2) If the side wall's thickness is not equal (valid for all the practical cases), this event can cause ray path errors that affect the sum of rays in the UTD method. | UTD solves the deficiency of the geometrical theory of diffraction (GTD) in the shadow boundary transition zone whereas keeping all of its advantages. |
| 3 SLOD-FDTD [49] | NM | By partitioning the problem space into pieces, and the suggested SLOD-FDTD approach minimizes computing resources. | The techniques deal with improving computational efficiency only. | The technique can be suitable to model electromagnetic waves in long tunnels. |
| 4 Split-Step-VPE [55] | NM | Provides the application feasibility of the parabolic equation method through a split-step parabolic equation (SSPE) mechanism. | The computed attenuation was not compared with other methods of computation-aiding mechanisms. | The validated results are promising for pedestrian tunnels. |
| 5 TDLC [57] | RT | This tunnel model includes the effect of the rolling stock, as the model is composed of the snapshots of the tunnel environments, which includes the number of rays, ray energy, and the delay of the ray. | TDL signals time-domain study is very restricted if the smallest delay is smaller than 8 ns (in this case, it will require enormous bandwidth (BW)). | With minimum 8 ns time delay due to multipath fading, the TDL model combines the multipath with minimum 60 dB power of a ray. |
| 6 AM [58] | RT | Asymptotic techniques such as ray tracing and ray launching are used to create a radio wave propagation model in straight arch-shaped tunnels. The interpolation of the normals of the facets was believed to reduce inaccuracy. | It lacks of adequate analytical analysis. | It presents a ray launching method that employs interpolation of the facets' normals to minimize the inaccuracy introduced by tessellation. This strategy allows us to see a convergence of outcomes by considering a vast number of factors. |
| 7 LRT [59] | | This method analytically proved the equivalence of the RT and the modal methods in the tunnel. | To maintain the equivalence, two conditions needed to be satisfied strictly: high frequency and long separation distances. | At high frequencies and long Tx-Rx separation distances, the ray tracing and modal methods exhibit equivalence behavior. |
| 8 WGMRT WG [63] | | The model uses an empirical propagation model, typically used in outside environments to find the tunnels' parameters. | The drawbacks of this method are that the parameter for one tunnel may not be applicable to another tunnel. | The advantage of this method is that, rather than a complex propagation mechanism, the received power and other parameters, such as the delay factor and K-factor, can be estimated quickly at the receiver. |

TABLE 4. (Continued.) Advantages and limitations of different propagation models.

| | | | | | |
|----|--------------|----|---|---|--|
| 9 | GJM [65] | SM | This method paves the way to mimic the real field radio wave propagation experiment in laboratory environment by building a prototype model of the real tunnel. | It may be time-consuming to develop a downscale version. | In the down-scaled model propagation was analyzed through numerical methods and ray tracing techniques, as well as by using WG-based models. |
| 10 | RDN [64] | SM | The proposed techniques have several benefits in estimating the total number of rays at the receiver end through several peripheral methods; ray-density normalization is essential. Thus, it solves the major problems of traditional geometrical optical means of power estimation at the receiver end. | A high number of traced rays uniformly dispersed in space is essential for the technique, which may not always be true for every tunnel. | This ray-optical approach is based on ray-density normalization instead of typical ray-optical methods that search for a single ray representing a local plane wavefront and can only address reflections at the plane of boundaries. To incorporate the curved boundary, many representations of each physical EM wave must exist concurrently. |
| 11 | EV [67] | NN | Using ray tracing or parabolic equation techniques, machine intelligence models may be trained to construct <i>electronic vision</i> to provide channel propagation based on an image or sequence with the geometric characteristics of the channel. Later, the tunnel's route loss exponent was estimated based on this vision, showing excellent results. | The demonstrated scenario was a simple in shape (rectangular tunnel) and it showed higher prediction error at near position close to transmitter. | Using a three-layer fully connected NN, the intelligent model outputs the path loss model's parameters by applying scalar functions with maximum and lowest properties, such as tunnel width, height, frequency, and permittivity. They used the stochastic gradient descent method for backpropagation, and the sum of squares is our loss function, aiming to decrease that as much as possible. |
| 12 | UQ [68] | NN | The results show that with a sufficient number of input dataset the uncertainty of fidelity measured data can be solved by applying this procedure. | The demonstrated results are at the frequency of less than 1 GHz, to test at higher frequency further test is required at higher frequency. | A sophisticated ANN is used to measure uncertainty in the input parameters of a VPE-based channel propagation model. A variable number of input configurations are used to train the six-layer ANN. The input data set was constructed using a VPE-based method. |
| 13 | ANN [66] | NN | This model has found some major possible problems with the application of ANN for tunnel wave propagation modeling: input, output, and ML model specification. The demonstrated results show that the ANN model outperforms in terms of accuracy, scalability, and interpreting the "physic's rule" through the ANN model. | The accuracy of this approach is close to the VPE method, but still, there exists an error, to match the predicted propagation signal power compared to the measured power. | When tested against both VPE-generated and measured data, the ANN's inference capabilities to unknown tunnel geometries were found to be solid. Furthermore, the network's scalability was excellent, allowing the ANN to maintain its precision even though the number of input features was increased. |
| 14 | MLNN [69] | NN | This multi-layer neural network can predict large-scale and small-scale fading in metro tunnels. | The training data set needs to be carefully collected as the relationship among the parameters are comparatively complex and the change in one parameter can affects the change in other parameter output [60, 16, 70, 71, 72]. | To use this technique it needs to carefully preprocess the data set such as removing outlier data, normalization. |

TABLE 4. (Continued.) Advantages and limitations of different propagation models.

| | | | | | |
|----|-------------------|------|--|---|---|
| 15 | FDTD-VPE [36] | N-N | This hybrid technique fuses the advantages of FDTD in obstructions or antenna regions with the straightforward computational benefits of VPE to simulate empty tunnels with along distance. It works in tunnels with antenna relays and obstacles. | The hybrid method was tested with a low frequency range of about 900 MHz. So, the methods need to be tested at a higher frequency range. | The VPE and FDTD techniques are conveniently applied to take advantage of the benefits of these methods, thus developing a fusion-based wave propagation technique for better prediction of received power inside tunnels. |
| 16 | SADI-FDTD [73] | N-N | It is a new method for modeling the propagation of electromagnetic waves through a giant tunnel. By segmenting the problem space, the recommended SADI-FDTD method prevents redundant computations. It permits the use of bigger cells in each segment. | This method applicability has not been tested for curved and branching tunnels with rough wall surfaces. | The SADI-FDTD method does not offer any mechanism to improve the prediction ability of the propagated wave in the tunnel, rather it just gives a mechanism to allow CPU execution time linearly whereas convention ADI-FDTD shows exponential behavior in this case. |
| 17 | VPE-WG [16] | N-N | Using VPE to figure out the size of the rectangular waveguide used in this technology makes it more flexible and resistant to changes in tunnel shape. | The overall execution time is reduced but the mean absolute error (MAE) is not improved significantly. | The performance of this method has not been verified at higher frequency more than 2 GHz. |
| 18 | VPE-RT [42] | N-RT | Reduce the complexity of RT through taking advantages of VPE. | The drawback of this technique is that no definite rules are specified for the interface grid to combine the RT and the VPE. | VPE is used to lengthy, generally uniform tunnel sections, whereas ray tracing is utilized in regions with complicated geometries and discontinuities. In this model, "Huygens surface" used as the interface space between RT and VPE. |
| | VPE-RT [76] | N-RT | In railway propagation studies, RT and VPE methods have been used a lot because they find a better balance between precision and reliability. | No straightforward mechanism was proposed for the <i>Huygens</i> interface location of plane. | Existing site-specific propagation models for tunnels and outdoor radio links are either hard to compute or make the predicted shape too simple. By combining RT and VPE, this trade-off between accuracy and speed might be avoided. RT is only used in parts of the channel that are geometrically complicated and not uniform, whereas VPE is used whenever its basic assumptions are met. |
| 19 | RT-FDTD [35] | N-RT | Ray tracing is used to evaluate a large area where the RT wave propagation mechanism is applied. In contrast, the FDTD technique can quickly analyze discontinuities in a tunnel environment. Thus, the combined technique enhances the accuracy and effectiveness of computational resources. | The consideration of the <i>virtual box</i> concept makes it too hard to deploy for general case model as in this model it needs to consider <i>virtual box</i> where any <i>discontinuity</i> type surface exists. | However, it has the problem that indoor structure computation needs to be done at the meter level more often. This strategy can be used in complex environments with no asymptotic solution. |

TABLE 4. (Continued.) Advantages and limitations of different propagation models.

| | | | | | |
|----|------------------|------|--|---|--|
| 20 | RT-graph [78] | N-RT | In this technique, hybrid ray tracing and graph channel model are used to consider the scattered points around principle paths vigorously representing the diffuse scattering components. | Scattering points are considered due to train body and the supporting pole in the vacant train. In realistic case, there may be other objects such as human, and other obstacles that the passenger. In that case, more complications needed to be considered. | The findings show essential reflected components may be identified and that up to two reflection bounces suffice for capturing principal multipath components (MPCs) via RT. Diffuse components provide 2–11 times as much power as specular components. |
| 21 | 2-BP [85] | BP | The model gives the analytical approach to find the breakpoint that help to deploy RT and the waveguide model in the tunnel. | The model needs further improvements as the measurement and this slope-based resulted signal did not match accurately. | The model is helpful in finding the breakpoint in a curvature tunnel, where the antenna gain does not affect the breakpoint. |
| 22 | SFF [15] | BP | When the curved form is approximated using planar facets, this approach allows the ray-launching method to be paired with interpolation of the normals of the facets. Because of this, it is an effective model for describing the movement of radio waves in straight, arch-shaped tunnels. | The model used a modified ray launching model in which the arch-shaped tunnel was approximated by the facets and a technique of interpolation of the facets' normals was achieved using the <i>Phong algorithm</i> [87], but it lacked extensive mathematical analysis. | The effect of transmitter-receiver location was investigated only with two alternate transmitter positions. |
| 23 | 4-slope [83] | BP | The model specifies a 4-slope propagation model in a long tunnel based on the carrier frequency, tunnel obstructions, and Tx and/or Rx location. | The proposed model was based on a heuristic approach, and it has not been analyzed with the established theory of wave propagation like waveguide propagation theory, ray optical models, and Maxwell's equations. | It divides the whole transmission path into four separate regions: the open space region, the near region, the distant region, and the excessively far region. |
| 24 | MIMO [89] | LS | considering spatial characteristics in 5G massive MIMO system models and provides guidelines to enhance the networks' accuracy in underground mobile communications. | The contribution analyzes the path loss using rectangular and cylindrical array antennae. There is no mechanism added to mitigate the near-end and the far-end disparity. | This contribution extensively analyzes the measured path loss in the tunnel with the MIMO system. |
| 25 | WG-SBR [90] | LS | It is claimed that the proposed model can predict path loss in cascaded trains with desirable accuracy and low complexity. | The model requires comparatively complex 3D-RT techniques, which is comparatively complicated. | They found the excess loss in the far-field region, which has a linear function of the path length of the tunnel curvature section. |
| 26 | Large-scale [92] | LS | This study gives the HST measured propagation parameters. | The effect of passengers on the train was not considered. | It finds out that the statistical propagation parameters vary in rural, viaduct or in the straight section. |
| | Large-scale [91] | LS | This study finds the modeling feasibility of HST channel with large-scale and small-scale models. | The models result in multiple slope variation of the path loss. The variations were not correlated with the channel diversity and other factors. | This study paves the way to find the slope variations of path loss in the tunnel i-th related factors. |

TABLE 4. (Continued.) Advantages and limitations of different propagation models.

| | | | | | |
|----|-----------|----|---|--|---|
| 27 | ISOA [93] | LS | This model showed better performance than the simple standard propagation model. In addition, it can mitigate the unwanted disparity waveguide effect at the far end and the near end. | The technique is tested at a frequency of 1.8 GHz. Therefore, to support a 5G network, it needs to test at the mmWave band. | The model can correct several parameters in contrast to the correction capacity was limited to 2 parameters [96]. |
| 28 | MFCT [71] | LS | Multi-frequency supporting capacity and defining the path loss in terms of the delay spread, frequency, and tunnel curvature. | There may be more additional parameters that can affect the path loss, but those were not considered in the proposal. | This neural network-based network can help design future-generation V2V channels. |
| 29 | TTI [94] | UC | In the subway line, the received signal strength was measured inside a moving train at 18 km/h, showing extensive penetration loss. The subway infrastructure facilities also have an immense influence on the received power. | The experimental frequency band is 2.6GHz; it needs to check the effects at higher frequencies. | This paper discusses the large-scale and small-scale fading of the propagated wave in the railway tunnel and concludes that the power spectral density function is wide at the receiver end (in train) because of several sources of Doppler effects. |
| 30 | HST [95] | UC | The 3-D ray tracer (RT) was calibrated to distinguish the multipath components (MPC) which are hardly distinguishable at small bandwidth and tested to investigate channel properties in various high-speed railway (HSR) environments. | Even though the method seems to be an effective way to predict the received power and other radio propagation characterization, it needs to convert the existing infrastructure into a 3-D drawing file. | The 3D-RT method came up with some conclusions, like the fact that more mobility means less coherence time and that the coherence bandwidth (100 MHz) changes in the opposite direction of the RMS delay spread. |

Disadvantage: Antenna location inside the train plays an important role in TTI communication.

Application: This model can be used in tunnels to communicate between moving vehicles and infrastructure.

b: HIGH SPEED TRAIN (HST)

This study [95] examined 5G mmWave channel characteristics for urban, rural, and tunnel high-speed rail (HSR) situations with straight and curved path configurations. Based on wideband tunnel measurements using the “mobile hotspot network” technology, 3D-RT parameters were calibrated by selecting the best results by feeding the simulation and measurement datasets. To iteratively minimize costs, a sophisticated calibration process based on a simulated annealing approach was used.

$$A(s) = \sum_{\tau=0}^{\tau_{max}} abs(|h_{rt}(s, \tau)|^2 - |h_m(s, \tau)|^2) \quad (19)$$

$$cost = \bar{A} \quad (20)$$

where s is the evaluated snapshots, τ is the excess delay and h_{rt} and h_m are the ray tracing simulation results and measurement channel impulse responses, respectively.

Advantage: The deployment of mmWave has been investigated, including different shapes of the tunnel (straight and curved) for high-speed train communication by updating the 3D-RT propagation modeling parameters with the measured data. The results indicate that the 3D-RT [31] calibrated model can generate a satisfactory attenuation level compared to the measured attenuation.

Disadvantage: The analytical insights of the proposed calibrated technique were not available, making its reliability in other systems difficult to determine or its implementation by other means challenging.

Application: To develop 5G infrastructure inside a tunnel for a high-speed train.

V. COMPARATIVE STUDY

This section compares the wave spreading model for indoor tunnels in terms of exceptional properties, characteristics, competitive advantages, and limitations. In Table 3, all the innovative procedures for determining propagation within the tunnel are listed. In Table 4, the benefits and drawbacks of different propagation techniques are listed. In Table 5, the existing models for wave propagation inside of tunnels are extensively compared in terms of various features, and characteristics.

TABLE 5. Characteristics of different propagation models. [M=measurement, S=simulation, B=measurement and simulation, U=unavailable, NF=not found].

| SL | Ref. | Tunnel specialty | Interface | M/S/B | Tunnel geometry | Reported frequency | Electrical Properties |
|----|---------------------|---|------------|-------|---|------------------------------|---|
| 1 | ADI-VPE [38] | lossy walls, transport tunnel | NF | B | straight, 3.5 km, rectangular, circular and arched cross-sections | 450-900 MHz, 2.1-10 GHz | straight: $\sigma_r=5$, $\sigma_0=0.01S_m$ |
| 2 | UTD [52, 53, 54] | Tunnel with cross junction | Modal-UTD | B | The main tunnel is 1.8 m wide and 2.4 m high, with an arched roof that starts 1.5 m up the side of the wall. The side tunnel is 1.5 m wide and 2.1 m high, with an arched roof that starts 1.4 m up the side of the wall. | 915, 2450, and 5800 MHz | NF |
| 3 | SLOD-FDTD [49] | 1. Straight, 2. cross junction tunnel, 3. curved tunnel | NF | B | 1. 3.336 km long, 8.3 m radius, 5.8 m (max) height, 2. 4.2 m wide, 3.0 m high, 3. 412.3 m, 6 m high, rectangular | GSM 900 MHz band | 1. $\sigma_r=2.5$, $\sigma_0=0.05S_m$; 2. $\sigma_r=10$, $\sigma_0=0.01 S_m$; 3. $\sigma_r=5.0$, $\sigma_0=0.0 1S_m$ |
| 4 | Split-Step-VPE [55] | Split-step Fourier transform | U | M | horseshoe-shape and box-shape tunnel. | 24 GHz | U |
| 5 | TDLC [57] | rectangular subway and high-speed rail tunnel | NF | S | rectangular tunnel (1) HSR: W=8.5 m, H=8.5 m, (2) subway: W=7.8, H=4.6 m | 2.4 GHz | consists of metal and concrete |
| 6 | AM [58] | semicircular, straight tunnel | NF | B | 3.336 km long, 8.3 m radius, 5.8 m (max) height | 5.8 GHz | NF |
| 7 | LRT [59] | straight concrete tunnel | NF | B | arched ceiling, cross-section is approximated by the equivalent rectangle of width (1.83 m) and a height of 2.35 m. | 455, 915, 2450, and 5800 MHz | NF |
| 8 | WGMRT [63] | straight train tunnel | NF | B | Semicircular shaped tunnel fitted in rectangular shape whose height is 4.9 m and width 6.9 m. | 24 GHz | NF |
| 9 | GJM [65] | straight tunnel | NF | B | straight tunnel, concrete walls, rectangular, height of 1.85 m, width of 1 m. | 1, 2.4, 10, 94 GHz | |
| 10 | RDN [64] | straight tunnel, circular tunnel | optics-RDN | B | concrete and stoneware, both rectangular and corrugated circular waveguide | 120 GHz | $\sigma_r=5$ (concrete), =8 (stoneware) |
| 11 | EV [67] | straight tunnel | NF | B | rectangular tunnel, width=7.8 m, height=5.3 m | 450 MHz, 900 MHz, 2100 MHz | $\sigma_r=5$ |
| 12 | UQ [68] | straight tunnel | NF | S | radius=2.5 m, height to central =1 m | 900 MHz | $\sigma_r=5$ |
| 13 | ANN [66] | straight tunnel | NF | B | height \approx 2.1 m, width \approx 2.1 m | 2.44 GHz | |

TABLE 5. (Continued.) Characteristics of different propagation models. [M=measurement, S=simulation, B=measurement and simulation, U=unavailable, NF=not found].

| | | | | | | | |
|----|----------------|--|-----------|-------|--|---|--|
| 14 | MLNN [69] | metro tunnel consisting straight and curved parts | U | B | rectangular part-28.1 m(L), 5.55 m(H); curved-100 m(L), 4.96 m(H); straight- 400 m(L), 4.96 m(H). | 5.6 GHz | U |
| 15 | FDTD-VPE [36] | straight rectangular tunnel | NF | S | height 2.4 m, width 1.8 m, long 80 m | 900 MHz | NF |
| 16 | SADI-FDTD [73] | semicircular, straight tunnel | ADI-FDTD | B | 3.336 km long, approximate area rectangle 8.3 m width and 5.8 m height | 2.4 GHz, 5.8 GHz | $\sigma_r=10$, $\sigma=0.01$ Sm |
| 17 | VPE-WG [16] | railway tunnel | VPE-WG | B | London’s subway features a 2.2-meter circle and 2.2- and 3.2-meter half-ellipses. The length is 550 meters and the height is 2.1 meters. Massif Central’s tunnel has a 4.3-meter radius and 1.8-meter flat base. | 900 MHz (Massif Central), 1 GHz, 2 GHz, 2440 MHz (London underground) | London Underground: $\sigma_r=5.5$, $\sigma=0.01$ Sm; Massif Central tunnel: $\sigma_r=5$, $\sigma=0.01$ Sm; |
| 18 | VPE-RT [76] | railway tunnel | VPE-RT | B | single track: W=5.4 m, H=5.2 m, L=40 m; Dual-track: 17.86 m, H=7.14 m, L=100 m; Station: W=17.86 m, H=7.17 m, L=123 m | 900 MHz | Massif Central tunnel: $\sigma_r=5$, $\sigma=0.01$ Sm; |
| | VPE-RT [76] | railway tunnel | VPE-RT | B | single track: W=5.4 m, H=5.2 m, L=40 m; Dual-track: 17.86 m, H=7.14 m, L=100m; Station: W=17.86 m, H=7.17 m, L=123 m | 900 MHz | Massif Central tunnel: $\sigma_r=5$, $\sigma=0.01$ Sm; |
| 19 | RT-FDTD [35] | metro train | RT-FDTD | B | The width (W), length (L), and height (H)are 2.2 m, 11.97 m, and 2.2 m, respectively | 26.5-40 GHz | |
| 20 | RT-graph [78] | railway tunnel | RT-graph | B | A 40-meter single-track tunnel is followed by a 100-meter dual-track tunnel; the railway station is 123 meters long. The railway station’s roof and side walls are made of metal. | 2450 MHz | Wall: $\sigma_r=5$, $\sigma=0.01$ Sm |
| SL | Ref. | Tunnel specialty | Interface | M/S/B | Tunnel geometry | Reported frequency | Electrical Properties |
| 21 | 2-BP [85] | 1:coal mine, 2:road, 3:potash mine, 4:arched-subway, 5:rectangular subway, 6: rail, 7:coal | NF | B | 1: 4X3.5, 2: 7.5X4, 3: 8.6X2.7, 4: 4.7X4.7, 5: 8.4X7.2, 6: 7.5X4, 7: 4X3.5 | 900 MHz, 915 MHz, 945 MHz, 1.853 GHz, 1800 MHz, 2.448 GHz | 1: $\sigma_r=10$, $\sigma=0.01$ Sm; 3: $\sigma_r=6$, $\sigma=0.0001$ m; 6: $\sigma_r=5.5$, $\sigma=0.01$ Sm |
| 22 | SFF [15] | two ways arched cross-section straight road tunnel | NF | B | 3.336 km long, 8.3 m radius, 5.8 m (max) height | 1 GHz, 2.4 GHz, 5.8 GHz, | $\sigma_r=10$, $\sigma=0.01$ Sm |

TABLE 5. (Continued.) Characteristics of different propagation models. [M=measurement, S=simulation, B=measurement and simulation, U=unavailable, NF=not found].

| | | | | | | | |
|----|------------------|---|------------------------|---|--|-----------------|----|
| 23 | 4-slope [83] | 1: pedestrians and cyclists arched tunnel; 2: dual carriageway road tunnel, tube shape | NF | M | 1: long 520 m, wide 4.7 m, height 4.5 m, walls and ceiling are of stone whereas the floor is asphalted, 2: width 3.75 m, height 4.70 m, flanked by a pair of 1 m wide pavements, length 7864 m | 400 MHz | NF |
| 24 | MIMO [89] | MIMO system | U | M | arched shaped tunnel | 3.5 GHz/160 MHz | U |
| 25 | WG-SBR [90] | joint channel model | in the curvature area | M | straight and cascaded train tunnel | 3.5 and 5.6 GHz | U |
| 26 | large-scale [92] | empirical model applied to HST tunnel. | not applicable | M | straight train tunnel connecting outside open parts. | 28 GHz/500 MHz | U |
| | Large-scale [91] | large-scale and small-scale models are applied to HST channel. | viaduct-tunnel-viaduct | M | straight train tunnel | 28 GHz/500 MHz | U |
| 27 | ISOA [93] | train tunnel with limited visibility and multiple reflection situations. | U | - | rectangular and arch-shaped train tunnel. | 1.8 GHz | U |
| 28 | MFCT [71] | tunnel with different curvature and different frequencies. | U | S | curved tunnel | 30 to 100 GHz | U |
| 29 | TTI [94] | subway tunnel | NF | M | long 100 m, velocity=18 km/h | 2.6 GHz | NF |
| 30 | HST [95] | express train in tunnel environments (straight-curved geometry) | NF | B | with straight and curved route shapes tunnels with normal dimensions, urban, and rural tunnel | 24-30 GHz | NF |

VI. RESEARCH SCOPE AND CHALLENGES

Even though there is extensive research on propagation inside a tunnel, there is still scope for further research. The main problems with developing a wave propagation model inside a tunnel are the different roughness of the side tunnels, which cause different penetration loss and scattering, wave propagation at mm wave frequency bands, and the lack of a localization system inside tunnels. This section gives a brief overview of six difficult issues that if solved will help researchers

and engineers in the field develop wave propagation models inside tunnels and other related areas.

A. CHARACTERIZATION OF PENETRATION LOSS

Defining the penetration loss induced by different materials inside the tunnels is essential. By calculating the loss caused by different layer materials, the penetration loss values in a particular obstruction layer between the transmitter and receiver may be determined. Because the amount of

electricity absorbed by the tunnel depends on the material, in this technique, the model determines the total route loss by adding the free-space path loss and the individual barrier penetration losses [97].

B. CHARACTERIZATION OF WAVE PROPAGATION AT HIGH FREQUENCY

As the lower frequency bands for radio communication are almost exhausted, we need to move to higher frequency bands for the proper operation of wireless communication networks. In [15], it was found that the dimension of the tunnel and the operating frequency are correlated.

C. CHARACTERIZATION OF INDOOR LOCALIZATION

There is a need to accurately predict the received power inside the tunnel for indoor localization service; the GPS system does not work as satellite signals cannot reach inside the tunnel. The necessity of localization inside the tunnel is also required for localizing robot or other purposes [98], [99]. The technology to develop indoor localization can be different data sources, but among these data sources, the received signal strength indicator signal is one of the important and easily usable techniques to create indoor localization facilities. A radio wave propagation prediction model can help develop the proper indoor localization system inside tunnels.

D. PROSPECTS OF APPLICATION OF GRAPH THEORY

In [100], electromagnetic wave propagation is modeled using graph theory. The fundamental concept of this graph theory-based propagation is established on the idea that in the tunnel, each node acts as the transmitter or the receiver and the edge of the graph indicates different propagation-related path loss or gain depending on what the case may be [101].

E. EFFECT OF HUMAN MOVEMENT INSIDE THE TUNNEL ON WAVE PROPAGATION

In [102], path loss was measured by considering humans, and in [103], the movement of humans along the aisle of a passenger train was considered on the path loss. Although [102], [103] extends the application of RT-graph theory including crowd and the non-crowded situation in the train.

F. USE OF AI TO MODEL WAVE PROPAGATION INSIDE TUNNEL

In the recent literature AI and deep learning are playing an important role to model different multi-variable and complicated systems outputs. In recent years, the possibility of deployment of an artificial neural network (ANN) has been expanded in diverse areas of interest. The natural phenomena and the rules of physics remain intact and govern the propagation of radio waves inside the tunnels. Although the usage of ANN to model radio wave propagation has been initiated [66], [67], [68], these contributions are not sufficient. To develop a well-optimized model by using ANN, we need to find the parameters that do not have an influence on the

propagated wave. Thus, a considerable number of probable parameters and a considerable real recorded database are required. Unfortunately, in an in-operation tunnel used for transportation such type of data collection is expensive. Therefore it is challenging to deploy ANN for modeling radio waves inside tunnels.

VII. CONCLUSION

In this study, we examined well-known and current academic resources of wave propagation for tunnels. Existing models have been categorized based on their development and formulation. We distinguish between this contribution and all previous surveys in Table 1. The propagation mechanisms were categorized based on the intrinsic wave propagation mechanism within tunnels. In our investigation, we analyzed thirty propagation mechanisms inside tunnels, ranging from the most basic to the most advanced ANN-based mechanisms. The results showed that tunnel structures and wall materials are different (since electrical properties have a big effect on how waves move). Owing to the scarcity of frequency bands for 5G and next-generation wireless mobile communication, the operational frequency should be moved to millimeter wave channels, where large bands are accessible. However, the deployment of this band inside tunnels has not been thoroughly investigated. The speed of the vehicles, the tunnels inside, and the building materials also have a big effect on how waves move through a transportation tunnel. The number of passengers in a vehicle can affect the nature of wave propagation. Considering all these aspects, certain models operate well under the conditions for which they were designed, but may not work well in other tunnel environments. Because of this, it is very important to define the wave propagation model for each tunnel through experimentation. We hope that this survey will inspire researchers to make a new tunnel propagation model, or that the study's comparisons will help them figure out which method is best for an empirical investigation.

REFERENCES

- [1] J. Boksiner, C. Chrysanthos, J. Lee, M. Billah, T. Bocskor, D. Barton, and J. Breakall, "Modeling of radiowave propagation in tunnels," in *Proc. IEEE Mil. Commun. Conf. (MILCOM)*, Oct. 2012, pp. 1–6, doi: [10.1109/MILCOM.2012.6415864](https://doi.org/10.1109/MILCOM.2012.6415864).
- [2] M. Liénard and P. Degauque, "Wideband analysis of propagation along radiating cables in tunnels," *Radio Sci.*, vol. 34, no. 1, pp. 113–122, Jan. 1999, doi: [10.1029/1998rs900007](https://doi.org/10.1029/1998rs900007).
- [3] M. A. Samad and D.-Y. Choi, "Analysis and modeling of propagation in tunnel at 3.7 and 28 GHz," *Comput., Mater. Continua*, vol. 71, no. 2, pp. 3127–3143, 2022, doi: [10.32604/cmc.2022.023086](https://doi.org/10.32604/cmc.2022.023086).
- [4] A. Hrovat, G. Kandus, and T. Javornik, "A survey of radio propagation modeling for tunnels," *IEEE Commun. Surveys Tuts.*, vol. 16, no. 2, pp. 658–669, 2nd Quart., 2014, doi: [10.1109/SURV.2013.091213.00175](https://doi.org/10.1109/SURV.2013.091213.00175).
- [5] T. Imai, "A survey of efficient ray-tracing techniques for mobile radio propagation analysis," *IEICE Trans. Commun.*, vol. E100.B, no. 5, pp. 666–679, 2017, doi: [10.1587/transcom.2016ebi0002](https://doi.org/10.1587/transcom.2016ebi0002).
- [6] T. K. Geok, F. Hossain, M. N. Kamaruddin, N. Z. Abd Rahman, S. Thiagarajah, A. Tan Wee Chiat, J. Hossen, and C. P. Liew, "A comprehensive review of efficient ray-tracing techniques for wireless communication," *Int. J. Commun. Antenna Propag. (IRECAP)*, vol. 8, no. 2, p. 123, Apr. 2018, doi: [10.15866/irecap.v8i2.13797](https://doi.org/10.15866/irecap.v8i2.13797).

- [7] M. E. Diago-Mosquera, A. Aragón-Zavala, and G. Castañón, "Bringing it indoors: A review of narrowband radio propagation modeling for enclosed spaces," *IEEE Access*, vol. 8, pp. 103875–103899, 2020, doi: [10.1109/ACCESS.2020.2999848](https://doi.org/10.1109/ACCESS.2020.2999848).
- [8] M. F. Iskander and Z. Yun, "Propagation prediction models for wireless communication systems," *IEEE Trans. Microw. Theory Techn.*, vol. 50, no. 3, pp. 662–673, Mar. 2002, doi: [10.1109/22.989951](https://doi.org/10.1109/22.989951).
- [9] C. Wang, Y. Yang, A. Ghazal, X. Ge, Y. Liu, and Y. Zhang, "Channel measurements and models for high-speed train wireless communication systems in tunnel scenarios: A survey," *SCIENTIA SINICA Informationis*, vol. 47, no. 10, pp. 1316–1333, Oct. 2017, doi: [10.1360/n112017-00089](https://doi.org/10.1360/n112017-00089).
- [10] H. Wei, G. Zheng, and M. Jia, "The measurements and simulations of millimeter wave propagation at 38 GHz in circular subway tunnels," in *Proc. China-Japan Joint Microw. Conf.*, Sep. 2008, pp. 51–54, doi: [10.1109/cjmw.2008.4772373](https://doi.org/10.1109/cjmw.2008.4772373).
- [11] X. Yang and Y. Lu, "Propagation characteristics of millimeter wave in circular tunnels," in *Proc. 7th Int. Symp. Antennas, Propag. EM Theory*, Oct. 2006, pp. 1–5, doi: [10.1109/ISAPE.2006.353508](https://doi.org/10.1109/ISAPE.2006.353508).
- [12] N. Uzunoglu and J. Kanellopoulos, "Scattering of a plane wave from cylindrical tunnels inside a lossy medium," in *Proc. Antennas Propag. Soc. Int. Symp.* Piscataway, NJ, USA: Institute of Electrical and Electronics Engineers, 1981, pp. 16–19, doi: [10.1109/APS.1981.1148466](https://doi.org/10.1109/APS.1981.1148466).
- [13] A. Aziminejad and Y. He, "Radio communication in curved tunnels: MIMO channel capacity for rail transit applications," *IEEE Veh. Technol. Mag.*, vol. 15, no. 1, pp. 99–106, Mar. 2020, doi: [10.1109/MVT.2019.2960590](https://doi.org/10.1109/MVT.2019.2960590).
- [14] J. S. Lamminmäki and J. J. A. Lempiäinen, "Radio propagation characteristics in curved tunnels," *IEE Proc. Microw., Antennas Propag.*, vol. 145, no. 4, p. 327, 1998, doi: [10.1049/ip-map:19981924](https://doi.org/10.1049/ip-map:19981924).
- [15] E. Masson, P. Combeau, M. Berbineau, R. Vauzelle, and Y. Pousset, "Radio wave propagation in arched cross section tunnels—Simulations and measurements," *J. Commun.*, vol. 4, no. 4, May 2009, doi: [10.4304/jcm.4.4.276-283](https://doi.org/10.4304/jcm.4.4.276-283).
- [16] X. Zhang, N. Sood, and C. D. Sarris, "Fast radio-wave propagation modeling in tunnels with a hybrid vector parabolic equation/waveguide mode theory method," *IEEE Trans. Antennas Propag.*, vol. 66, no. 12, pp. 6540–6551, pp. 1–10, Dec. 2018, doi: [10.1109/TAP.2018.2864344](https://doi.org/10.1109/TAP.2018.2864344).
- [17] L. Ding, T. Yin, and H. Zhu, "Wave propagation in a periodic jointed tunnel model," in *Analysis, Design, and Construction of Tunnels and Underground Structures*. Reston, VA, USA: American Society of Civil Engineers, Jun. 2014, pp. 9–16, doi: [10.1061/9780784478479.002](https://doi.org/10.1061/9780784478479.002).
- [18] C. Zhou and J. Waynert, "Modeling and measurement of radio propagation in rectangular tunnels at low frequencies," in *Proc. IEEE Antennas Propag. Soc. Int. Symp. (APSURSI)*, Jul. 2014, pp. 253–254, doi: [10.1109/APS.2014.6904458](https://doi.org/10.1109/APS.2014.6904458).
- [19] X. Liu, X. Yin, and G. Zheng, "Experimental investigation of millimeter-wave MIMO channel characteristics in tunnel," *IEEE Access*, vol. 7, pp. 108395–108399, 2019, doi: [10.1109/ACCESS.2019.2932576](https://doi.org/10.1109/ACCESS.2019.2932576).
- [20] B. Jacard and O. Maldonado, "Microwave modeling of rectangular tunnels," *IEEE Trans. Microw. Theory Techn.*, vol. MTT-32, no. 6, pp. 576–581, Jun. 1984, doi: [10.1109/TMTT.1984.1132731](https://doi.org/10.1109/TMTT.1984.1132731).
- [21] M. Nilsson, J. Slettenmark, and C. Beckman, "Wave propagation in curved road tunnels," in *Proc. IEEE Antennas Propag. Soc. Int. Symp. Digest. Antennas, Gateways Global Network. Held Conjoint USNC/URSI Nat. Radio Sci. Meeting*, Jun. 1998, pp. 21–26, doi: [10.1109/APS.1998.701569](https://doi.org/10.1109/APS.1998.701569).
- [22] X. Zhang and C. D. Sarris, "Rigorous statistical modeling of propagation in tunnels with rough surface walls," in *Proc. IEEE Int. Symp. Antennas Propag. USNC/URSI Nat. Radio Sci. Meeting*, Jul. 2018, pp. 1751–1752, doi: [10.1109/APUSNCURSINRSM.2018.8608649](https://doi.org/10.1109/APUSNCURSINRSM.2018.8608649).
- [23] J. Lee and H. L. Bertoni, "Coupling at cross, T, and L junctions in tunnels and urban street canyons," *IEEE Trans. Antennas Propag.*, vol. 51, no. 5, pp. 926–935, May 2003, doi: [10.1109/TAP.2003.811461](https://doi.org/10.1109/TAP.2003.811461).
- [24] X. Yang and Y. Lu, "Research on propagation characteristics of millimeter wave in tunnels," *Int. J. Infr. Millim. Waves*, vol. 28, no. 10, pp. 901–909, Jul. 2007, doi: [10.1007/s10762-007-9268-y](https://doi.org/10.1007/s10762-007-9268-y).
- [25] M. Celaya-Echarri, L. Azpilicueta, P. Lopez-Iturri, I. Picallo, E. Aguirre, J. J. Astrain, J. Villadangos, and F. Falcone, "Radio wave propagation and WSN deployment in complex utility tunnel environments," *Sensors*, vol. 20, no. 23, p. 6710, Nov. 2020, doi: [10.3390/s20236710](https://doi.org/10.3390/s20236710).
- [26] Y. Yamaguchi, T. Abe, and T. Sekiguchi, "Radio wave propagation loss in the VHF to microwave region due to vehicles in tunnels," *IEEE Trans. Electromagn. Compat.*, vol. 31, no. 1, pp. 87–91, Feb. 1989, doi: [10.1109/15.19912](https://doi.org/10.1109/15.19912).
- [27] H. Jiang, Z. Zhang, L. Wu, J. Dang, and G. Gui, "A 3-D non-stationary wideband geometry-based channel model for MIMO vehicle-to-vehicle communications in tunnel environments," *IEEE Trans. Veh. Technol.*, vol. 68, no. 7, pp. 6257–6271, Jul. 2019, doi: [10.1109/TVT.2019.2918333](https://doi.org/10.1109/TVT.2019.2918333).
- [28] H. Jiang, Z. Chen, J. Zhou, J. Dang, and L. Wu, "A general 3D non-stationary wideband twin-cluster channel model for 5G V2V tunnel communication environments," *IEEE Access*, vol. 7, pp. 137744–137751, 2019, doi: [10.1109/ACCESS.2019.2942442](https://doi.org/10.1109/ACCESS.2019.2942442).
- [29] *Ray Optics Simulation*. Accessed: Apr. 21, 2021. [Online]. Available: <https://tricktu288.github.io/ray-optics/>
- [30] *Wireless InSite 3D Wireless Prediction Software*. Accessed: Apr. 21, 2021. [Online]. Available: <https://www.remcom.com/wireless-insite-em-propagation-software>
- [31] *CloudRT*. Accessed: Apr. 21, 2021. [Online]. Available: <http://www.raytracer.cloud/>
- [32] L. Ma, K. Guan, D. Yan, D. He, B. Ai, J. Kim, and H. Chung, "Characterization for high-speed railway channel enabling smart rail mobility at 22.6 GHz," in *Proc. IEEE Wireless Commun. Netw. Conf. (WCNC)*, May 2020, pp. 1–6, doi: [10.1109/WCNC45663.2020.9120474](https://doi.org/10.1109/WCNC45663.2020.9120474).
- [33] L. Ma, K. Guan, D. Yan, D. He, N. R. Leonor, B. Ai, and J. Kim, "Satellite-terrestrial channel characterization in high-speed railway environment at 22.6 GHz," *Radio Sci.*, vol. 55, no. 3, pp. 1–15, Mar. 2020, doi: [10.1029/2019rs006995](https://doi.org/10.1029/2019rs006995).
- [34] H. Liu, J. Liang, K. Chen, and T. Liao, "Wireless channel simulation and measurement of maglev tunnel," in *Proc. 3rd Inf. Commun. Technol. Conf. (ICTC)*, May 2022, pp. 25–32, doi: [10.1109/ICTC55111.2022.9778779](https://doi.org/10.1109/ICTC55111.2022.9778779).
- [35] Y. Wang, S. Safavi-Naeini, and S. K. Chaudhuri, "A hybrid technique based on combining ray tracing and FDTD methods for site-specific modeling of indoor radio wave propagation," *IEEE Trans. Antennas Propag.*, vol. 48, no. 5, pp. 743–754, May 2000, doi: [10.1109/8.855493](https://doi.org/10.1109/8.855493).
- [36] W. Hou, J. Wang, and Y. Li, "A hybrid method of FDTD and vector parabolic equation for radio wave propagation prediction in tunnels," in *Proc. IEEE Int. Symp. Antennas Propag. USNC/URSI Nat. Radio Sci. Meeting*, Jul. 2017, pp. 1639–1640, doi: [10.1109/APUSNCURSINRSM.2017.8072862](https://doi.org/10.1109/APUSNCURSINRSM.2017.8072862).
- [37] X. Zhang and C. D. Sarris, "Error analysis and comparative study of numerical methods for the parabolic equation applied to tunnel propagation modeling," *IEEE Trans. Antennas Propag.*, vol. 63, no. 7, pp. 3025–3034, Jul. 2015, doi: [10.1109/TAP.2015.2421974](https://doi.org/10.1109/TAP.2015.2421974).
- [38] R. Martelly and R. Janaswamy, "An ADI-PE approach for modeling radio transmission loss in tunnels," *IEEE Trans. Antennas Propag.*, vol. 57, no. 6, pp. 1759–1770, Jun. 2009.
- [39] R. Martelly and R. Janaswamy, "Modeling radio transmission loss in curved, branched and rough-walled tunnels with the ADI-PE method," *IEEE Trans. Antennas Propag.*, vol. 58, no. 6, pp. 2037–2045, Jun. 2010, doi: [10.1109/TAP.2010.2046862](https://doi.org/10.1109/TAP.2010.2046862).
- [40] J. C. Strikwerda, *Finite Difference Schemes and Partial Differential Equations*, 2nd ed. Philadelphia, PA, USA: SIAM, Jan. 2004.
- [41] X. Zhang and C. D. Sarris, "A high-accuracy ADI scheme for the vector parabolic equation applied to the modeling of wave propagation in tunnels," *IEEE Antennas Wireless Propag. Lett.*, vol. 13, pp. 650–653, 2014, doi: [10.1109/LAWP.2014.2313737](https://doi.org/10.1109/LAWP.2014.2313737).
- [42] X. Zhang, N. Sood, J. Siu, and C. D. Sarris, "Efficient propagation modeling in railway environments using a hybrid vector parabolic equation/ray-tracing method," in *Proc. IEEE Int. Symp. Antennas Propag. USNC/URSI Nat. Radio Sci. Meeting*, Jul. 2015, pp. 1680–1681, doi: [10.1109/APS.2015.7305229](https://doi.org/10.1109/APS.2015.7305229).
- [43] X. He, D. Li, J. Wang, and S. Li, "A new ADI-PE scheme with fourth-order accuracy for radio wave propagation prediction in tunnels," in *Proc. Int. Symp. Antennas Propag. Conf.*, Dec. 2014, pp. 259–260, doi: [10.1109/ISANP.2014.7026629](https://doi.org/10.1109/ISANP.2014.7026629).
- [44] W. Hou, D. Li, J. Wang, and X. He, "A wide angle 3D ADI-PE scheme for radio wave propagation prediction in tunnels," in *Proc. IEEE 6th Int. Symp. Microw., Antenna, Propag., EMC Technol. (MAPE)*, Oct. 2015, pp. 205–208, doi: [10.1109/MAPE.2015.7510299](https://doi.org/10.1109/MAPE.2015.7510299).
- [45] P. Bernardi, D. Caratelli, R. Cicchetti, V. Schena, and O. Testa, "A numerical scheme for the solution of the vector parabolic equation governing the radio wave propagation in straight and curved rectangular tunnels," *IEEE Trans. Antennas Propag.*, vol. 57, no. 10, pp. 3249–3257, Oct. 2009, doi: [10.1109/TAP.2009.2027142](https://doi.org/10.1109/TAP.2009.2027142).

- [46] N. Noori, S. Safavi-Naeini, and H. Oraizi, "A new three-dimensional vector parabolic equation approach for modeling radio wave propagation in tunnels," in *Proc. IEEE Antennas Propag. Soc. Int. Symp.*, Jul. 2005, pp. 3–8, doi: [10.1109/APS.2005.1552810](https://doi.org/10.1109/APS.2005.1552810).
- [47] X. Zhang, N. Sood, and C. D. Sarris, "Propagation modeling in complex tunnel environments: A comparison of vector parabolic equation and ray-tracing solutions," in *Proc. Int. Conf. Electromagn. Adv. Appl. (ICEAA)*, Sep. 2017, pp. 1676–1679, doi: [10.1109/ICEAA.2017.8065614](https://doi.org/10.1109/ICEAA.2017.8065614).
- [48] H. F. Rasool, M. A. Qureshi, A. Aziz, and F. H. Malik, "Efficient solution of Noye–Hayman implicit finite-difference method for modelling wave propagation in tunnels," *Electron. Lett.*, vol. 56, no. 22, pp. 1167–1169, Sep. 2020, doi: [10.1049/el.2020.1978](https://doi.org/10.1049/el.2020.1978).
- [49] M. M. Rana and A. S. Mohan, "Segmented-locally-one-dimensional-FDTD method for EM propagation inside large complex tunnel environments," *IEEE Trans. Magn.*, vol. 48, no. 2, pp. 223–226, Feb. 2012, doi: [10.1109/TMAG.2011.2177075](https://doi.org/10.1109/TMAG.2011.2177075).
- [50] A. V. Popov and N. Y. Zhu, "Modeling radio wave propagation in tunnels with a vectorial parabolic equation," *IEEE Trans. Antennas Propag.*, vol. 48, no. 9, pp. 1403–1412, Sep. 2000, doi: [10.1109/8.898773](https://doi.org/10.1109/8.898773).
- [51] X. Zhang and C. D. Sarris, "Vector parabolic equation modeling of wireless propagation in tunnels with statistically rough surface walls," in *Proc. Int. Appl. Comput. Electromagn. Soc. Symp. (ACES)*, Mar. 2018, pp. 1–2, doi: [10.23919/ROPACES.2018.8364122](https://doi.org/10.23919/ROPACES.2018.8364122).
- [52] Y. Hwang, Y. P. Zhang, and R. G. Kouyoumjian, "Ray-optical prediction of radio-wave propagation characteristics in tunnel environments. 1. Theory," *IEEE Trans. Antennas Propag.*, vol. 46, no. 9, pp. 1328–1336, Sep. 1998, doi: [10.1109/8.719976](https://doi.org/10.1109/8.719976).
- [53] Y. P. Zhang, Y. Hwang, and R. G. Kouyoumjian, "Ray-optical prediction of radio-wave propagation characteristics in tunnel environments. 2. Analysis and measurements," *IEEE Trans. Antennas Propag.*, vol. 46, no. 9, pp. 1337–1345, Sep. 1998, doi: [10.1109/8.719977](https://doi.org/10.1109/8.719977).
- [54] C. Zhou, R. Jacksha, and M. Reyes, "Measurement and modeling of radio propagation from a primary tunnel to cross junctions," in *Proc. IEEE Radio Wireless Symp. (RWS)*, Jan. 2016, pp. 70–72, doi: [10.1109/RWS.2016.7444368](https://doi.org/10.1109/RWS.2016.7444368).
- [55] H. Qin and X. Zhang, "Modeling of millimeter-wave propagation in tunnels with split-step parabolic equation method," in *Proc. IEEE-APS Topical Conf. Antennas Propag. Wireless Commun. (APWC)*, Sep. 2022, pp. 60–62, doi: [10.1109/APWC49427.2022.9899947](https://doi.org/10.1109/APWC49427.2022.9899947).
- [56] Z. Yun and M. F. Iskander, "Ray tracing for radio propagation modeling: Principles and applications," *IEEE Access*, vol. 3, pp. 1089–1100, 2015, doi: [10.1109/ACCESS.2015.2453991](https://doi.org/10.1109/ACCESS.2015.2453991).
- [57] H. Qiu, J. M. Garcia-Loygorri, K. Guan, D. He, Z. Xu, B. Ai, and M. Berbineau, "Emulation of radio technologies for railways: A tapped-delay-line channel model for tunnels," *IEEE Access*, vol. 9, pp. 1512–1523, 2021, doi: [10.1109/access.2020.3046852](https://doi.org/10.1109/access.2020.3046852).
- [58] E. Masson, P. Combeau, Y. Cocheril, M. Berbineau, L. Aveneau, and R. Vauzelle, "Radio wave propagation in arch-shaped tunnels: Measurements and simulations by asymptotic methods," *Comp. Rendus Phys.*, vol. 11, no. 1, pp. 44–53, Jan. 2010, doi: [10.1016/j.crhy.2009.12.003](https://doi.org/10.1016/j.crhy.2009.12.003).
- [59] C. Zhou and J. Waynert, "The equivalence of the ray tracing and modal methods for modeling radio propagation in lossy rectangular tunnels," *IEEE Antennas Wireless Propag. Lett.*, vol. 13 pp. 615–618, 2014, doi: [10.1109/LAWP.2014.2313312](https://doi.org/10.1109/LAWP.2014.2313312).
- [60] Z. Sun and I. F. Akyildiz, "Channel modeling and analysis for wireless networks in underground mines and road tunnels," *IEEE Trans. Commun.*, vol. 58, no. 6, pp. 1758–1768, Jun. 2010, doi: [10.1109/TCOMM.2010.06.080353](https://doi.org/10.1109/TCOMM.2010.06.080353).
- [61] C. Zhou, "Ray tracing and modal methods for modeling radio propagation in tunnels with rough walls," *IEEE Trans. Antennas Propag.*, vol. 65, no. 5, pp. 2624–2634, May 2017, doi: [10.1109/TAP.2017.2677398](https://doi.org/10.1109/TAP.2017.2677398).
- [62] J. A. Castiblanco, D. Seetharamdoo, M. Berbineau, and M. Ney, "Modal wave propagation characteristics in tunnels of different cross sections," in *Proc. 10th Eur. Conf. Antennas Propag. (EuCAP)*, Apr. 2016, pp. 1–4, doi: [10.1109/EuCAP.2016.7481738](https://doi.org/10.1109/EuCAP.2016.7481738).
- [63] A. González-Plaza, C. Calvo-Ramírez, C. Briso-Rodríguez, J. Moreno García-Loygorri, D. Oliva, and J. I. Alonso, "Propagation at mmW band in metropolitan railway tunnels," *Wireless Commun. Mobile Comput.*, vol. 2018, pp. 1–10, Mar. 2018, doi: [10.1155/2018/7350494](https://doi.org/10.1155/2018/7350494).
- [64] D. Didascalou, T. M. Schafer, F. Weinmann, and W. Wiesbeck, "Ray-density normalization for ray-optical wave propagation modeling in arbitrarily shaped tunnels," *IEEE Trans. Antennas Propag.*, vol. 48, no. 9, pp. 1316–1325, Sep. 2000, doi: [10.1109/8.898764](https://doi.org/10.1109/8.898764).
- [65] J. Gerasimov, N. Balal, E. Liokumovitch, Y. Richter, M. Gerasimov, E. Bamani, G. A. Pinhasi, and Y. Pinhasi, "Scaled modeling and measurement for studying radio wave propagation in tunnels," *Electronics*, vol. 10, no. 1, p. 53, Dec. 2020, doi: [10.3390/electronics10010053](https://doi.org/10.3390/electronics10010053).
- [66] A. Seretis, X. Zhang, K. Zeng, and C. D. Sarris, "Artificial neural network models for radiowave propagation in tunnels," *IET Microw., Antennas Propag.*, vol. 14, no. 11, pp. 1198–1208, Jul. 2020, doi: [10.1049/iet-map.2019.0988](https://doi.org/10.1049/iet-map.2019.0988).
- [67] A. Malone and C. D. Sarris, "Electromagnetic vision: Machine intelligence models of radiowave propagation in tunnels," in *Proc. IEEE Int. Symp. Antennas Propag. USNC/URSI Nat. Radio Sci. Meeting*, Jul. 2018, pp. 557–558, doi: [10.1109/APUSNCURSINRSM.2018.8608893](https://doi.org/10.1109/APUSNCURSINRSM.2018.8608893).
- [68] A. Seretis, X. Zhang, and C. D. Sarris, "Uncertainty quantification of radio propagation models using artificial neural networks," in *Proc. IEEE Int. Symp. Antennas Propag. USNC-URSI Radio Sci. Meeting*, Jul. 2019, pp. 229–230, doi: [10.1109/APUSNCURSINRSM.2019.8888357](https://doi.org/10.1109/APUSNCURSINRSM.2019.8888357).
- [69] J. Qian, A. Saleem, and G. Zheng, "Channel modeling based on multi-layer artificial neural network in metro tunnel environments," *ETRI J.*, Oct. 2022, pp. 1–13, doi: [10.4218/etrij.2022-0101](https://doi.org/10.4218/etrij.2022-0101).
- [70] C. Briso-Rodríguez, P. Fratilesco, and Y. Xu, "Path loss modeling for train-to-train communications in subway tunnels at 900/2400 MHz," *IEEE Antennas Wireless Propag. Lett.*, vol. 18, no. 6, pp. 1164–1168, Jun. 2019, doi: [10.1109/LAWP.2019.2911406](https://doi.org/10.1109/LAWP.2019.2911406).
- [71] M. Zhai, K. Zhai, H. Cui, and D. Li, "Multifrequency channel characterization for curved tunnels," *IEEE Antennas Wireless Propag. Lett.*, vol. 20, no. 12, pp. 2457–2460, Dec. 2021, doi: [10.1109/LAWP.2021.3114553](https://doi.org/10.1109/LAWP.2021.3114553).
- [72] C. Wang, W. Ji, G. Zheng, and A. Saleem, "Analysis of propagation characteristics for various subway tunnel scenarios at 28 GHz," *Int. J. Antennas Propag.*, vol. 2021, pp. 1–16, Sep. 2021, doi: [10.1155/2021/7666624](https://doi.org/10.1155/2021/7666624).
- [73] M. M. Rana, M. S. Anwar, and M. A. Motin, "Segmentation technique with ADI-FDTD for EM propagation modeling in electrically large structure," in *Proc. Int. Conf. Electr. Eng. Inf. Commun. Technol.*, Apr. 2014, pp. 1–4, doi: [10.1109/ICEEICT.2014.6919159](https://doi.org/10.1109/ICEEICT.2014.6919159).
- [74] F. Hossain, T. Geok, T. Rahman, M. Hindia, K. Dimiyati, C. Tso, and M. Kamaruddin, "A smart 3D RT method: Indoor radio wave propagation modelling at 28 GHz," *Symmetry*, vol. 11, no. 4, p. 510, Apr. 2019, doi: [10.3390/sym11040510](https://doi.org/10.3390/sym11040510).
- [75] M. M. Taygur and T. F. Eibert, "A ray-tracing algorithm based on the computation of (exact) ray paths with bidirectional ray-tracing," *IEEE Trans. Antennas Propag.*, vol. 68, no. 8, pp. 6277–6286, Aug. 2020, doi: [10.1109/TAP.2020.2983775](https://doi.org/10.1109/TAP.2020.2983775).
- [76] X. Zhang, N. Sood, J. K. Siu, and C. D. Sarris, "A hybrid ray-tracing/vector parabolic equation method for propagation modeling in train communication channels," *IEEE Trans. Antennas Propag.*, vol. 64, no. 5, pp. 1840–1849, May 2016, doi: [10.1109/TAP.2016.2535125](https://doi.org/10.1109/TAP.2016.2535125).
- [77] C. Pfeiffer and A. Grbic, "Metamaterial Huygens' surfaces: Tailoring wave fronts with reflectionless sheets," *Phys. Rev. Lett.*, vol. 110, no. 19, May 2013, Art. no. 197401, doi: [10.1103/PhysRevLett.110.197401](https://doi.org/10.1103/PhysRevLett.110.197401).
- [78] D. He, K. Guan, J. M. Garcia-Loygorri, B. Ai, X. Wang, C. Zheng, C. Briso-Rodríguez, and Z. Zhong, "Channel characterization and hybrid modeling for millimeter-wave communications in metro train," *IEEE Trans. Veh. Technol.*, vol. 69, no. 11, pp. 12408–12417, Nov. 2020, doi: [10.1109/TVT.2020.3023153](https://doi.org/10.1109/TVT.2020.3023153).
- [79] M. A. Samad, F. D. Diba, and D.-Y. Choi, "A survey of rain attenuation prediction models for terrestrial links—Current research challenges and state-of-the-art," *Sensors*, vol. 21, no. 4, p. 1207, Feb. 2021, doi: [10.3390/s21041207](https://doi.org/10.3390/s21041207).
- [80] K. Guan, B. Ai, Z. Zhong, C. F. Lopez, L. Zhang, C. Briso-Rodríguez, A. Hrovat, B. Zhang, R. He, and T. Tang, "Measurements and analysis of large-scale fading characteristics in curved subway tunnels at 920 MHz, 2400 MHz, and 5705 MHz," *IEEE Trans. Intell. Transp. Syst.*, vol. 16, no. 5, pp. 2393–2405, Oct. 2015, doi: [10.1109/TITS.2015.2404851](https://doi.org/10.1109/TITS.2015.2404851).
- [81] N. Faruk, I. Y. Abdurashed, N. T. Surajudeen-Bakinde, E. Adetiba, A. A. Oloyede, A. Abdulkarim, O. S. Sowande, A. H. Ifijeh, and A. A. Atayero, "Large-scale radio propagation path loss measurements and predictions in the VHF and UHF bands," *Heliyon*, vol. 7, no. 6, Jun. 2021, Art. no. e07298, doi: [10.1016/j.heliyon.2021.e07298](https://doi.org/10.1016/j.heliyon.2021.e07298).
- [82] K. Guan, Z. Zhong, J. I. Alonso, and C. Briso-Rodríguez, "Measurement of distributed antenna systems at 2.4 GHz in a realistic subway tunnel environment," *IEEE Trans. Veh. Technol.*, vol. 61, no. 2, pp. 834–837, Feb. 2012, doi: [10.1109/TVT.2011.2178623](https://doi.org/10.1109/TVT.2011.2178623).
- [83] A. Hrovat, G. Kandus, and T. Javornik, "Four-slope channel model for path loss prediction in tunnels at 400 MHz," *IET Microw., Antennas Propag.*, vol. 4, no. 5, p. 571, 2010, doi: [10.1049/iet-map.2009.0159](https://doi.org/10.1049/iet-map.2009.0159).

- [84] H. Xia, H. L. Bertoni, L. R. Maciel, A. Lindsay-Stewart, and R. Rowe, "Radio propagation characteristics for line-of-sight microcellular and personal communications," *IEEE Trans. Antennas Propag.*, vol. 41, no. 10, pp. 1439–1447, Oct. 1993, doi: [10.1109/8.247785](https://doi.org/10.1109/8.247785).
- [85] Y. P. Zhang, "Novel model for propagation loss prediction in tunnels," *IEEE Trans. Veh. Technol.*, vol. 52, no. 5, pp. 1308–1314, Sep. 2003, doi: [10.1109/TVT.2003.816647](https://doi.org/10.1109/TVT.2003.816647).
- [86] S. K. Kalyankar, Y. H. Lee, and Y. S. Meng, "Two-slope path loss model for curved-tunnel environment with concept of break point," *IEEE Trans. Intell. Transp. Syst.*, vol. 22, no. 12, pp. 7850–7859, Dec. 2021, doi: [10.1109/ITITS.2020.3012724](https://doi.org/10.1109/ITITS.2020.3012724).
- [87] A. S. Glassner, *Principles of Digital Image Synthesis*. San Mateo, CA, USA: Morgan Kaufmann, 2014.
- [88] S. Jiang, J. Song, W. Wang, and R. Ibrahim, "A study on radio propagation channel modelling for tunnels," in *Proc. 16th Eur. Conf. Antennas Propag. (EuCAP)*, Mar. 2022, pp. 1–4, doi: [10.23919/EuCAP53622.2022.9769562](https://doi.org/10.23919/EuCAP53622.2022.9769562).
- [89] A. Saleem, H. Cui, Y. He, and A. Boag, "Channel propagation characteristics for massive multiple-input/multiple-output systems in a tunnel environment [measurements corner]," *IEEE Antennas Propag. Mag.*, vol. 64, no. 3, pp. 126–142, Jun. 2022, doi: [10.1109/map.2022.3162807](https://doi.org/10.1109/map.2022.3162807).
- [90] J. Qian, Y. Wu, A. Saleem, and G. Zheng, "Path loss model for 3.5 GHz and 5.6 GHz bands in cascaded tunnel environments," *Sensors*, vol. 22, no. 12, p. 4524, Jun. 2022, doi: [10.3390/s22124524](https://doi.org/10.3390/s22124524).
- [91] J.-J. Park, J. Lee, K.-W. Kim, and M.-D. Kim, "Large- and small-scale fading characteristics of mmWave HST propagation channel based on 28-GHz measurements," in *Proc. 15th Eur. Conf. Antennas Propag. (EuCAP)*, Mar. 2021, pp. 1–5, doi: [10.23919/EuCAP51087.2021.9411172](https://doi.org/10.23919/EuCAP51087.2021.9411172).
- [92] J. Park, J. Lee, K. Kim, H. Kwon, and M. Kim, "Empirical millimeter-wave wideband propagation characteristics of high-speed train environments," *ETRI J.*, vol. 43, no. 3, pp. 377–388, Jun. 2021, doi: [10.4218/etrij.2020-0239](https://doi.org/10.4218/etrij.2020-0239).
- [93] Y. Zheng, R. Yan, and Y. Liu, "Correction of radio wave propagation prediction model based on improved seagull algorithm in tunnel environment," *IEEE Access*, vol. 9, pp. 149569–149581, 2021, doi: [10.1109/ACCESS.2021.3122300](https://doi.org/10.1109/ACCESS.2021.3122300).
- [94] T. Domínguez-Bolaño, J. Rodríguez-Piñeiro, J. A. García-Naya, X. Yin, and L. Castedo, "Measurement-based characterization of train-to-infrastructure 2.6 GHz propagation channel in a modern subway station," *IEEE Access*, vol. 6, pp. 52814–52830, 2018, doi: [10.1109/ACCESS.2018.2870564](https://doi.org/10.1109/ACCESS.2018.2870564).
- [95] D. He, B. Ai, K. Guan, Z. Zhong, B. Hui, J. Kim, H. Chung, and I. Kim, "Channel measurement, simulation, and analysis for high-speed railway communications in 5G millimeter-wave band," *IEEE Trans. Intell. Transp. Syst.*, vol. 19, no. 10, pp. 3144–3158, Oct. 2018, doi: [10.1109/ITITS.2017.2771559](https://doi.org/10.1109/ITITS.2017.2771559).
- [96] K. Rizk, J. F. Wagen, and F. Gardiol, "Influence of database accuracy on two-dimensional ray-tracing-based predictions in urban microcells," *IEEE Trans. Veh. Technol.*, vol. 49, no. 2, pp. 631–642, Mar. 2000, doi: [10.1109/25.832995](https://doi.org/10.1109/25.832995).
- [97] A. Deshmukh and S. K. Bodhe, "Characterization of radio propagation at 60 GHz channel," in *Proc. 1st Asian Himalayas Int. Conf. Internet*, Nov. 2009, pp. 1–8, doi: [10.1109/AHICI.2009.5340281](https://doi.org/10.1109/AHICI.2009.5340281).
- [98] W. Zhen and S. Scherer, "Estimating the localizability in tunnel-like environments using LiDAR and UWB," in *Proc. Int. Conf. Robot. Autom. (ICRA)*, May 2019, doi: [10.1109/ICRA.2019.8794167](https://doi.org/10.1109/ICRA.2019.8794167).
- [99] T. Seco, M. T. Lázaro, J. Espelósín, L. Montano, and J. L. Villarroel, "Robot localization in tunnels: Combining discrete features in a pose graph framework," *Sensors*, vol. 22, no. 4, p. 1390, Feb. 2022, doi: [10.3390/s22041390](https://doi.org/10.3390/s22041390).
- [100] R. Adeogun, T. Pedersen, C. Gustafson, and F. Tufvesson, "Polarimetric wireless indoor channel modeling based on propagation graph," *IEEE Trans. Antennas Propag.*, vol. 67, no. 10, pp. 6585–6595, Oct. 2019, doi: [10.1109/TAP.2019.2925128](https://doi.org/10.1109/TAP.2019.2925128).
- [101] M. Gan, G. Steinbock, Z. Xu, T. Pedersen, and T. Zemen, "A hybrid ray and graph model for simulating vehicle-to-vehicle channels in tunnels," *IEEE Trans. Veh. Technol.*, vol. 67, no. 9, pp. 7955–7968, Sep. 2018, doi: [10.1109/TVT.2018.2839980](https://doi.org/10.1109/TVT.2018.2839980).
- [102] P. Tang, "Path loss in metro train in mm-Wave band with consideration of human body effect," in *Proc. 7th Int. Conf. Comput. Commun. (ICCC)*, Dec. 2021, pp. 1010–1014, doi: [10.1109/ICCC54389.2021.9674629](https://doi.org/10.1109/ICCC54389.2021.9674629).
- [103] F. Lu, K. Yunoki, and N. Suzuki, "Influence of human body movement on mm Wave communication in bullet train cars," in *Proc. IEEE Int. Conf. Ubiquitous Wireless Broadband (ICUWB)*, Oct. 2016, pp. 1–4, doi: [10.1109/ICUWB.2016.7790517](https://doi.org/10.1109/ICUWB.2016.7790517).



MD. ABDUS SAMAD (Member, IEEE) received the Ph.D. degree in information and communication engineering from Chosun University, Gwangju, South Korea. He worked as an Assistant Professor at the Department of Electronics and Telecommunication Engineering, International Islamic University Chittagong, Chattogram, Bangladesh, from 2013 to 2017. He is currently working as an Assistant Professor at the Department of Information and Communication Engineering, Yeungnam University, South Korea. His research interests include signal processing, antenna design, electromagnetic wave propagation, applications of artificial neural networks, deep learning, and millimeter-wave propagation by interference or atmospheric causes for 5G and beyond wireless networks. He won the Prestigious Korean Government Scholarship (GKS) for his Ph.D. study.



SUNG-WOONG CHOI (Senior Member, IEEE) received the B.S. and M.S. degrees in electronic engineering from Kyungbook National University, South Korea, in 1997 and 1999, respectively, and the Ph.D. degree from the Department of Information and Communication Engineering, Korea Advanced Institute of Science and Technology, South Korea, in 2019. He is currently a Principal Member of the Electronics and Telecommunications Research Institute. His research interests include wireless communications, antenna/propagation, and EMI/EMC.



CHUNG-SUP KIM received the B.S. and M.S. degrees in electrical engineering from Kyung-pook National University, Daegu, South Korea, in 1997 and 1999, respectively. Since 1999, he has been with the Electronics and Telecommunications Research Institute as a Principal Researcher. His research interests include direction finding, beamforming, RADAR, radio propagation, and 5G communication.



KWONHWE CHOI (Senior Member, IEEE) received the B.S., M.S., and Ph.D. degrees in electronic and electrical engineering from the Pohang University of Science and Technology, Pohang, South Korea, in 1994, 1996, and 2000, respectively. From 2000 to 2003, he worked with the Electronics and Telecommunications Research Institute, Daejeon, South Korea, as a Senior Research Staff Member. In 2003, he joined the Department of Information and Communication Engineering, Yeungnam University, Gyeongsan, South Korea, where he is currently a Professor. He has authored a textbook on *Problem-Based Learning in Communication Systems Using MATLAB and Simulink* (Wiley, 2016). His research interests include signal design for communication systems, multiple access schemes, diversity schemes for wireless fading channels, multiple antenna systems, and in-band full-duplex systems.